

Supplementary Material

Hierarchical Subcomponent Self-Assembly of Covalent Triple-stranded Complex with 3d-4f Vertices: Luminescence and Magnetic Property

Zhi Liu,^{a,b} Fan Yin,^{a,b} Jian Yang,^b Xiao-Qing Guo,^b Li-Peng Zhou,^b Chong-Bin Tian^{*a,b} and Qing-Fu-Sun^{*a,b}

a. College of Chemistry, Fuzhou University, Fuzhou 350108, People's Republic of China

b. Fujian College, University of Chinese Academy of Sciences, Fuzhou 350002, People's Republic of China.

* Correspondence to: tianchongbin@fjirsm.ac.cn; qfsun@fjirsm.ac.cn

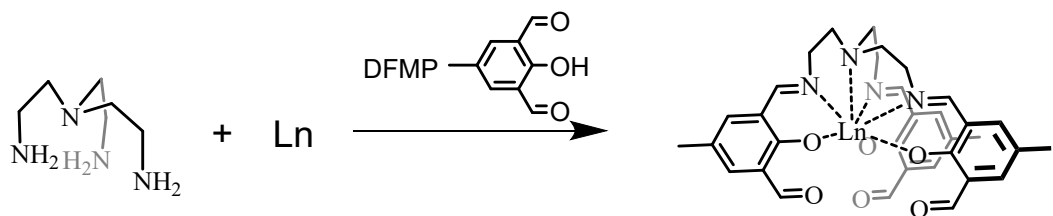
Table of contents

1. General	2
2. Synthesis Procedures of ligands 1-Ln (Ln=Sm, Eu, Yb, Lu)	3
3. Self-assembly and characterization of 3a-3c-(Ln, Zn) and 3^{a'}-(Dy, Co) assemblies.	5
4. UV-Vis and FL spectrum	24
5. Magnetic Data	32
6. Single crystal X-ray diffraction studies.....	33
7. Continuous shape measurements analysis	42
7. Reference.....	44

1. General

All chemicals and solvents were purchased from commercial companies and used without further purification. Anhydrous solvents were distilled according to standard procedures. Deuterated solvents were purchased from Admas and Sigma-Aldrich, 1D and 2D-NMR spectra were measured on a Bruker Biospin Avanced III (400 MHz) spectrometer. ¹H-NMR chemical shifts were determined with respect to residual signals of the deuterated solvents used. ESI-MS spectra of **3a-3c-(Gd, Zn)** were recorded on LC-QTOF-MS (G6520B), while ESI-TOF-MS spectra of other compounds were recorded on an Impact II UHRTOF mass spectrometry from Bruker, with tuning mix as the internal standard. Data analysis was conducted with the Bruker Data Analysis software (Version 4.3) and simulations were performed with the Bruker Isotope Pattern software and Thermo Xcalibur Qual Browser software (Thermo Foundation 2.0). UV-vis spectra are recorded on UV-2700 UV-vis spectrophotometer from SHIMADZU. Excitation and emission spectra were recorded on the FS5 spectrofluorometer from Edinburg Photonics. Power X-Ray diffraction (P-XRD) data were collected using Miniflex600 (Cu - K α radiation: $\lambda = 1.54056 \text{ \AA}$) in the range of $5^\circ < 2\theta < 40^\circ$. Unless otherwise specified, all experiments have been carried out at room temperature (298 K). Thermogravimetric analyses were performed using a GA/NETZSCH STA449C instrument heated from 30–1200 °C (heating rate of 10 °C min⁻¹, nitrogen stream). Elemental analyses of C, H, and N were measured using a Vario EL III elemental analyzer. Magnetic data were collected with a Quantum Design MPMS XL superconducting quantum interference device (SQUID) magnetometer. Diamagnetic corrections were made using Pascal's constants. The empirical molecular formula for **3a'-(Dy, Co)** was determined according to the results of element analyses and TGA data.

2. Synthesis Procedures of ligands 1-Ln (Ln=Sm, Eu, Yb, Lu)



Scheme S1. The synthetic route of 1-Ln

The compounds of 2,6-Diformyl-p-cresol (DFMP), **1-Dy**, **1-Yb** and **1-Lu** were synthesized following the literature procedure^{1,2}.

Synthesis of ligands **1-Eu**.

The synthetic progress of **1-Eu** is the same as that of **1-Sm** except that Eu(NO₃)₃·6H₂O (326 mg, 0.73 mmol) was used. ¹H NMR (400 MHz, DMSO-*d*₆) δ 7.87 (s, 1H), 5.77 (s, 1H), 4.41 (s, 1H), 1.21 (s, 3H), -1.60 ~ -2.04 (m, 2H), -2.53 ~ -3.08 (m, 2H), -16.63 (s, 1H). ESI-MS: calcd. for [M+Na]⁺: 757.1508, found 757.1496.

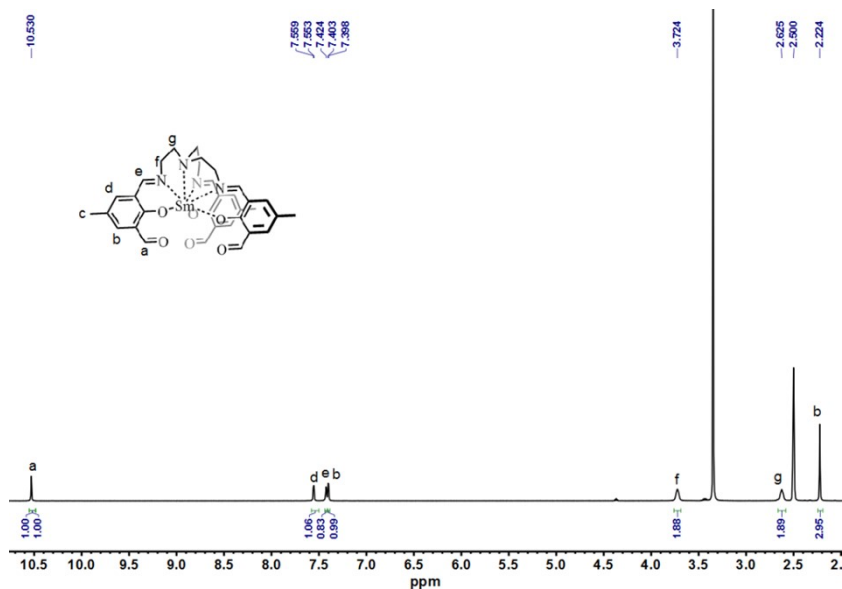


Figure S1. ¹H NMR spectrum of **1-Sm** (400 MHz, DMSO-*d*₆, 298 K).

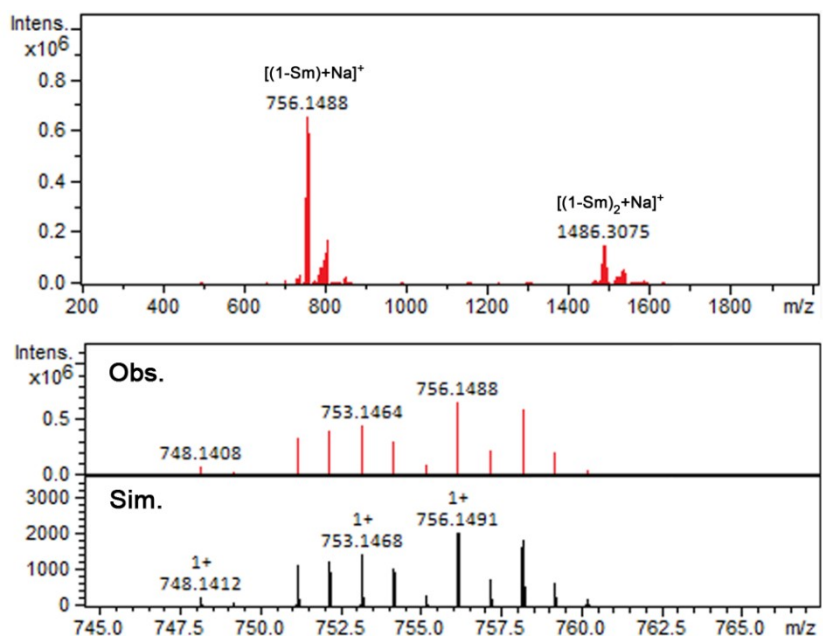


Figure S2. ESI-TOF-MS spectrum of **1-Sm** with insets showing the observed and simulated isotopic patterns of the +1 peak.

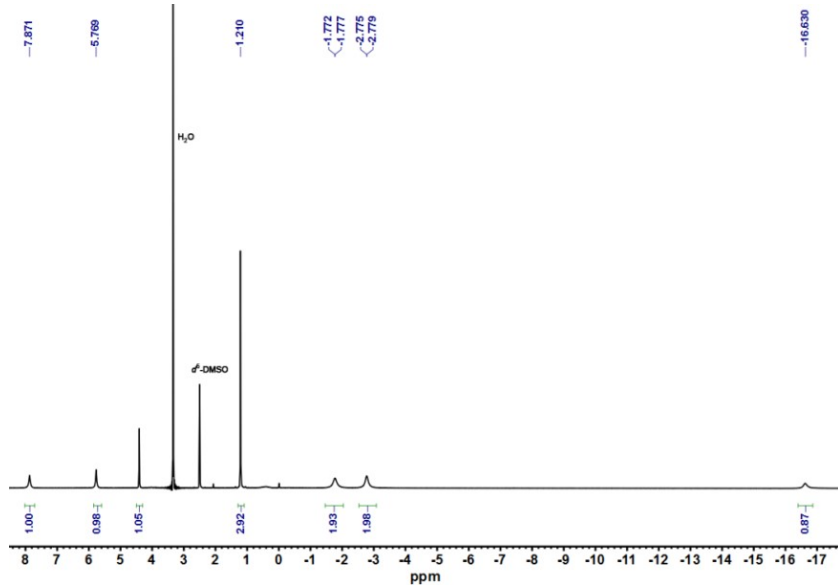


Figure S3. ${}^1\text{H}$ NMR spectrum of **1-Eu** (400 MHz, $\text{DMSO}-d_6$, 298 K).

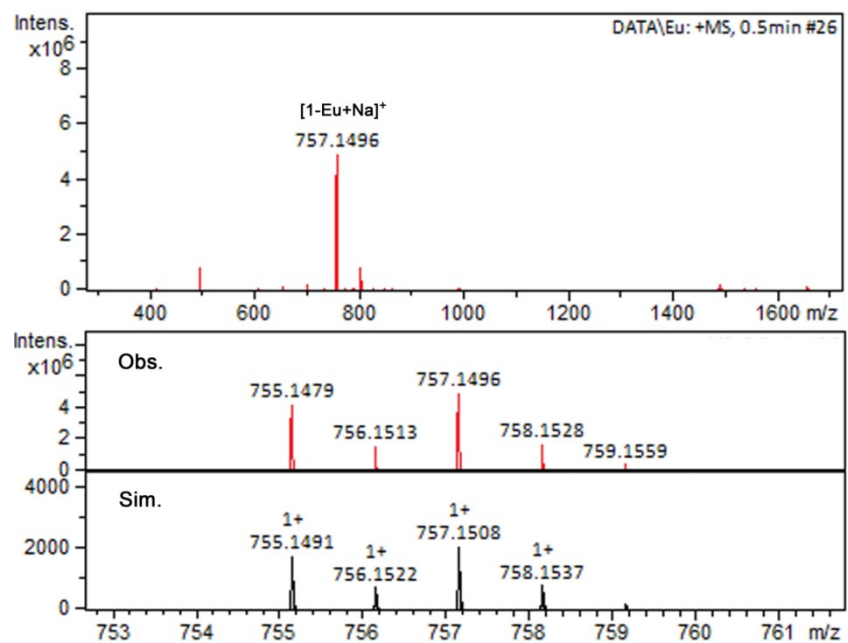


Figure S4. ESI-TOF-MS spectrum of **1-Eu** with insets showing the observed and simulated isotopic patterns of the +1 peak.

3. Self-assembly and characterization of 3a-3b-(Ln, Zn) and 3a'-(Dy, Co) assemblies.

The synthesis procedure of 3a-(Sm, Zn) is in the text.

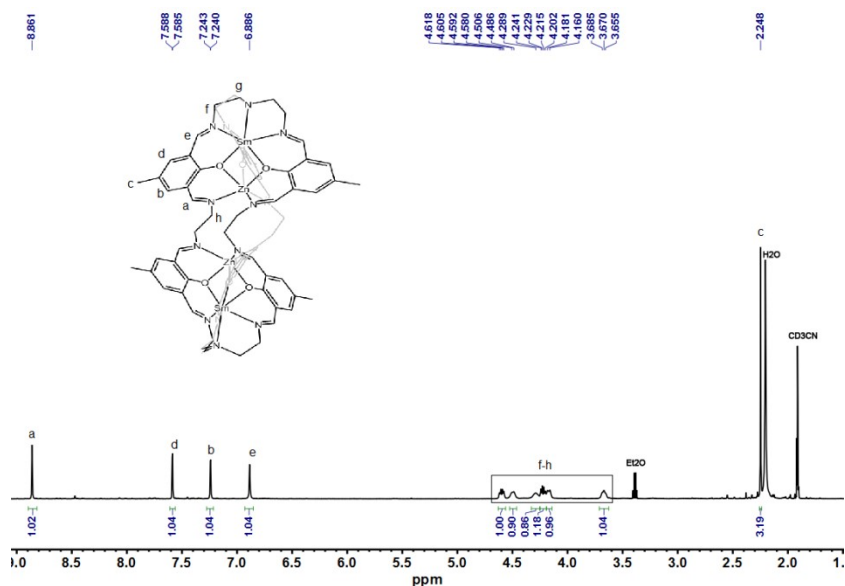


Figure S5. ^1H NMR spectrum of **3a-(Sm, Zn)** (400 MHz, CD_3CN , 298 K).

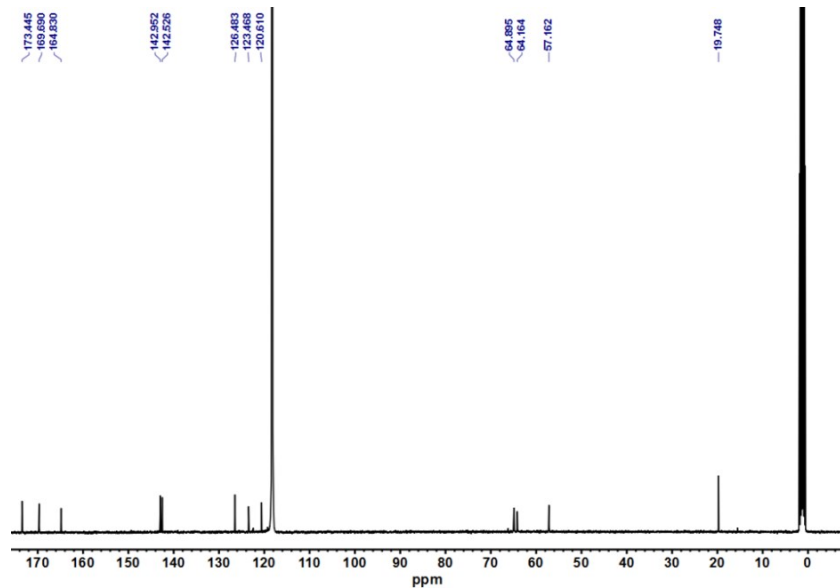


Figure S6. ^{13}C NMR spectrum of **3a-(Sm, Zn)** (101 MHz, CD_3CN , 298 K).

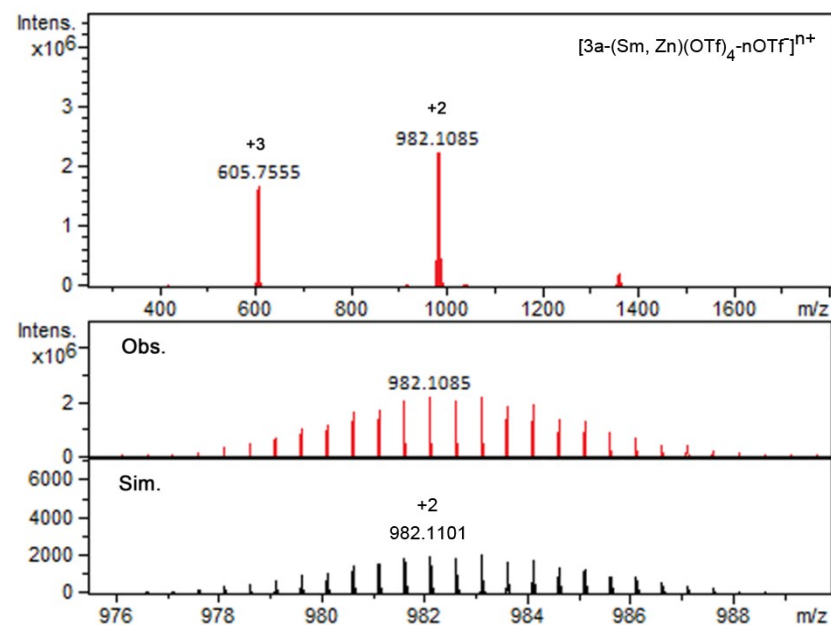


Figure S7. ESI-TOF-MS spectrum of **3a-(Sm, Zn)** with insets showing the observed and simulated isotopic patterns of the +2 peak.

3a-(Eu, Zn): The synthetic progress of **3a-(Eu, Zn)** is similar with the procedure of **3a-(Sm, Zn)**. ^1H NMR (400 MHz, CD_3CN) δ 7.53 (s, 1H), 6.29 (s, 1H), 4.92 (s, 1H), 1.90 (s, 3H), 1.56 – 1.36 (m, 1H), -0.02 ~ -0.25 (m, 1H), -3.33 ~ -5.48 (m, 2H), -10.37 (s, 1H), -21.62 (s, 1H). ESI-TOF-MS for **3a-(Eu, Zn)**: the following picked signals are those at the highest intensities. m/z calcd. for $[\text{3a-(Eu, Zn)}(\text{OTf})_2]^{2+}$ 984.1116, found 984.1092; calcd. for $[\text{3a-(Eu, Zn)}(\text{OTf})_1]^{3+}$ 606.4236, found 606.4230.

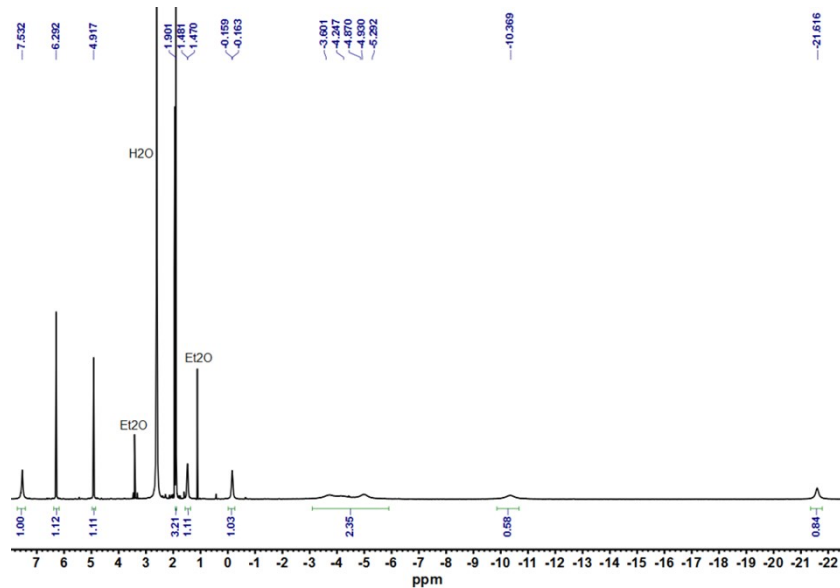


Figure S8. ¹H NMR spectrum of **3a-(Eu, Zn)** (400 MHz, CD₃CN, 298 K).

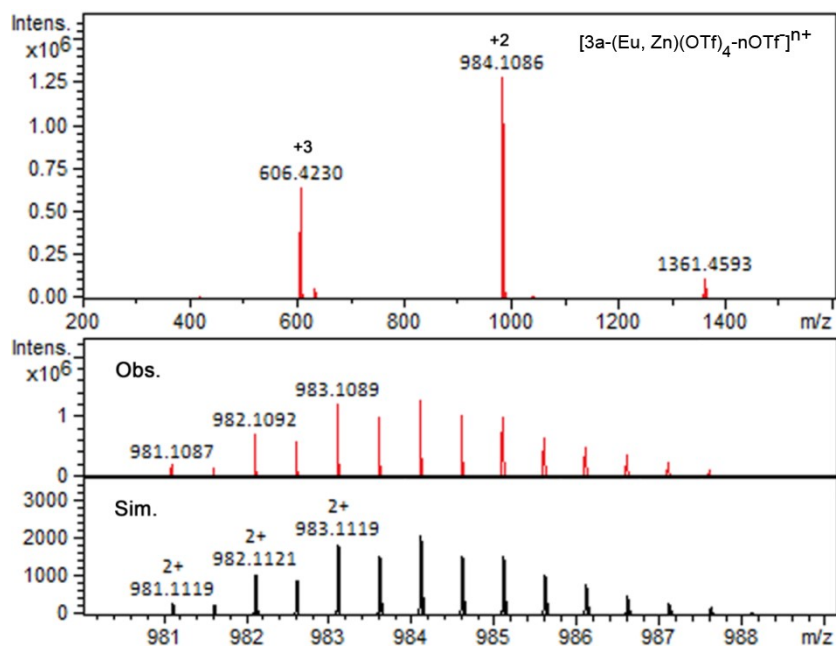


Figure S9. ESI-TOF-MS spectrum of **3a-(Eu, Zn)** with insets showing the observed and simulated isotopic patterns of the +2 peak.

3a-(Yb, Zn): The synthetic progress of **3a-(Yb, Zn)** is similar with the procedure of **3a-(Sm, Zn)**. ESI-TOF-MS for **3a-(Yb, Zn)**: the following picked signals are those at the highest intensities. *m/z* calcd. for [3a-(Yb, Zn)(OTf)₂]²⁺ 1005.1296, found 1005.1275; calcd. for [3a-(Yb, Zn)(OTf)₁]³⁺ 620.4356, found 620.4342.

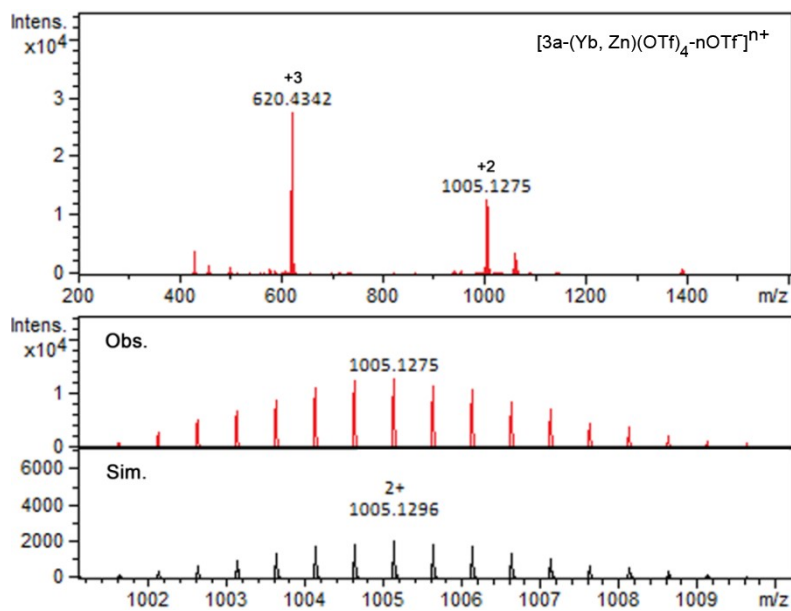


Figure S10. ESI-TOF-MS spectrum of **3a**-(Yb, Zn) with insets showing the observed and simulated isotopic patterns of the $+2$ peak.

3a-(Lu, Zn): The synthetic progress of **3a-(Lu, Zn)** is similar with the procedure of **3a-(Sm, Zn)**. ^1H NMR (400 MHz, CD_3CN) δ 8.50 (s, 1H), 8.31 (s, 1H), 7.53 (d, $J = 1.7$ Hz, 1H), 7.40 (d, $J = 1.7$ Hz, 1H), 3.90 (td, 1H), 3.77 ~ 3.70 (m, 1H), 3.68 (s, 2H), 3.36 ~ 3.26 (m, 1H), 2.95 (td, $J = 9.1, 4.7$ Hz, 1H), 2.31 (s, 3H). ESI-TOF-MS for **3a-(Lu, Zn)**: the following picked signals are those at the highest intensities. m/z calcd. for $[\text{3a-(Lu, Zn)}(\text{OTf})_2]^{2+}$ 1007.1304, found 1007.1304; calcd. for $[\text{3a-(Lu, Zn)}(\text{OTf})_1]^{3+}$ 621.7703, found 621.7695.

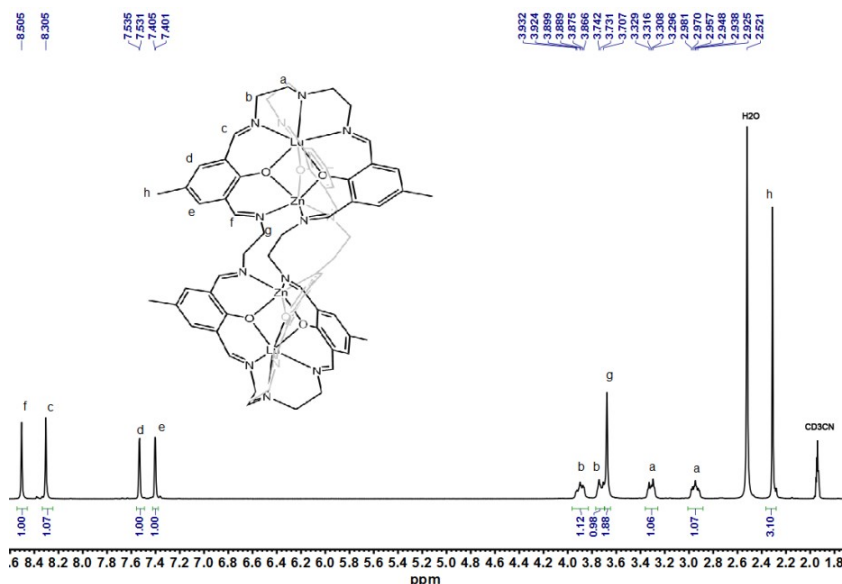


Figure S11. ^1H NMR spectrum of **3a**-(Lu, Zn) (400 MHz, CD_3CN , 298 K).

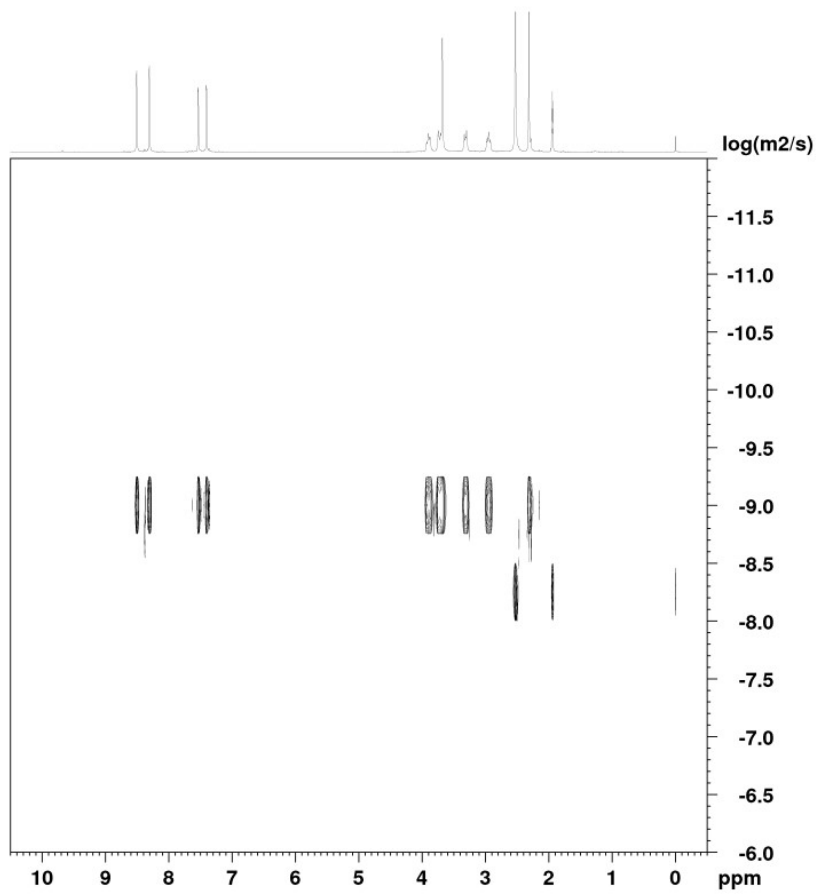


Figure S12. ¹H DOSY NMR spectrum of **3a-(Lu, Zn)** (400 MHz, CD₃CN, 298K).

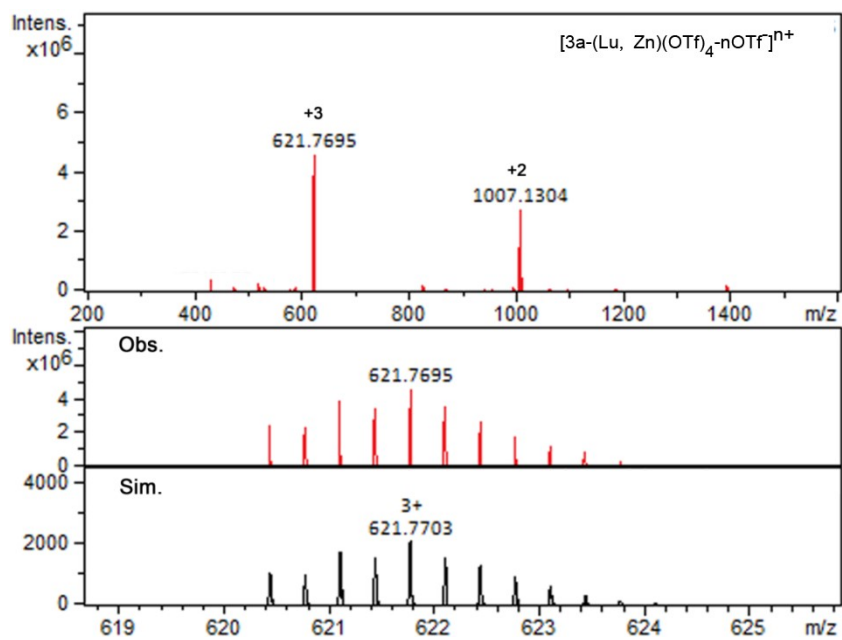


Figure S13. ESI-TOF-MS spectrum of **3a-(Lu, Zn)** with insets showing the observed and simulated isotopic patterns of the +3 peak.

3a-(Gd, Zn): The synthetic progress of **3a-(Gd, Zn)** is similar with the procedure of **3a-(Sm, Zn)**. ESI-TOF-MS for **3a-(Gd, Zn)**: the following picked signals are those at the highest intensities. *m/z* calcd. for $[3\text{a-(Gd, Zn)}(\text{OTf})_2]^{2+}$ 989.11, found 989.11; calcd. for $[3\text{a-(Gd, Zn)}(\text{OTf})_1]^{3+}$ 609.76, found 609.76.

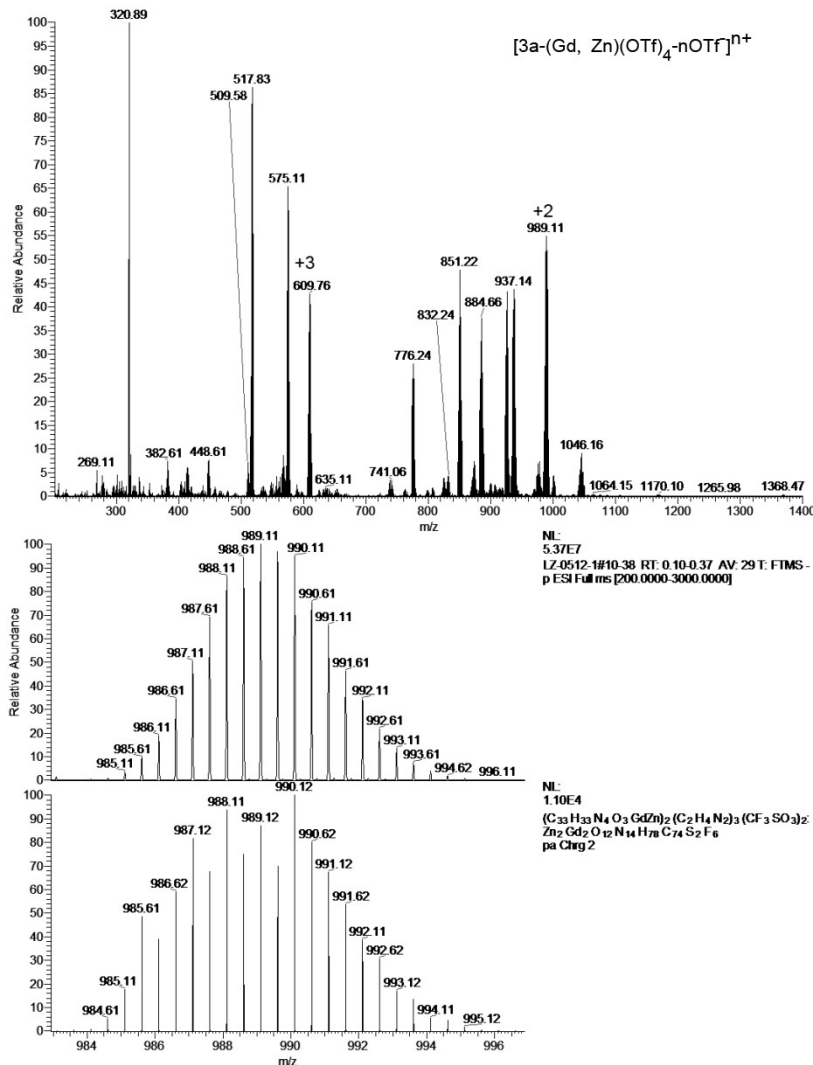


Figure S14. ESI-TOF-MS spectrum of **3a-(Gd, Zn)** with insets showing the observed and simulated isotopic patterns of the +2 peak.

3a'-(Dy, Co): The synthetic progress of **3a'-(Dy, Co)** is the same as that of Synthesis of **3a-(Sm, Zn)** except that **1-Dy** and $\text{Co}(\text{OTf})_2$ were used. ESI-TOF-MS: calcd. for $[3\text{a'-(Dy, Co)}(\text{OTf})_2]^{2+}$: 988.1250, found 988.1240; calcd. $[3\text{a'-(Dy, Co)}(\text{OTf})_1]^{3+}$: 609.0992, found 609.0986. Anal. calcd. for $\text{C}_{82}\text{H}_{89}\text{N}_{17}\text{O}_{19}\text{S}_4\text{F}_{12}\text{Dy}_2\text{Co}_2$ (2415.24): C 40.74; H 3.71; N 9.86; found: C 40.70; H 3.833; N 9.83.

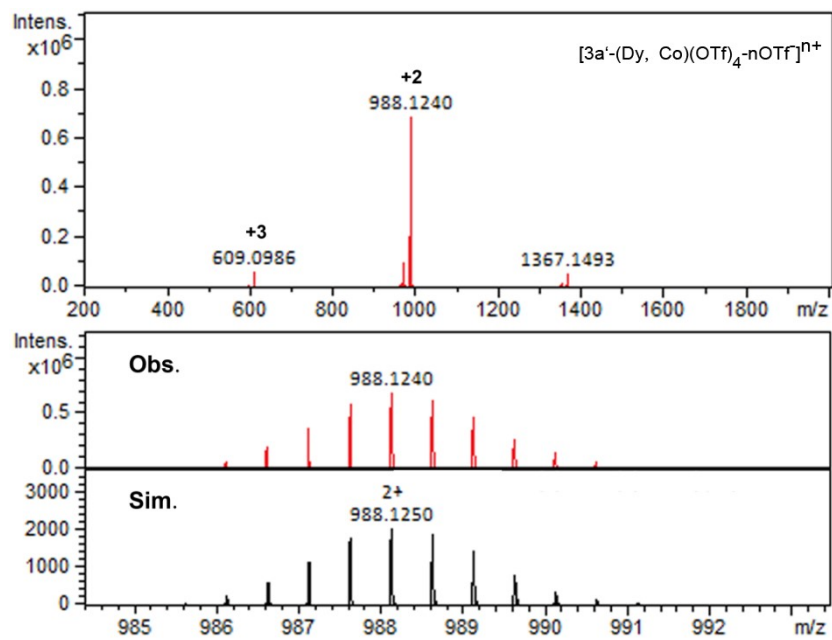


Figure S15. ESI-TOF-MS spectrum of $3a'-(\text{Dy, Co})$ with insets showing the observed and simulated isotopic patterns of the +2 peak.

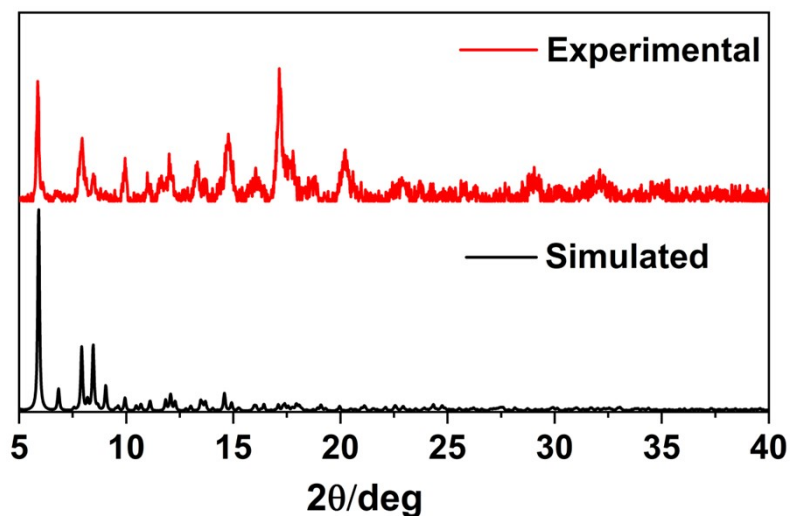


Figure S16. PXRD data of $3a'-(\text{Dy, Co})$.

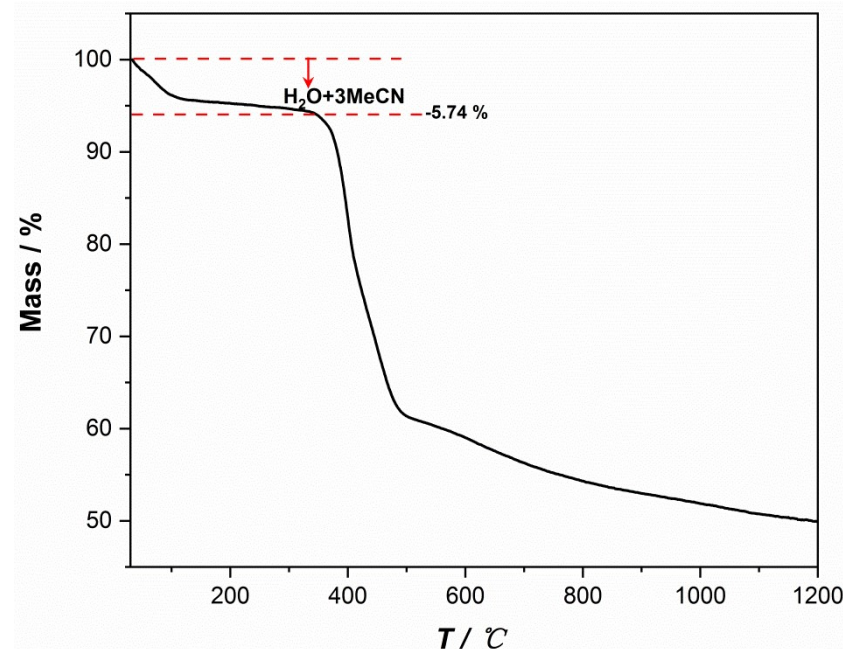


Figure S17. TG profiles for complex **3a'-(Dy, Co)**.

The self-assembly reactions of **3b-3c-(Ln, Zn)** were proceeded in similar procedures as **3a-(Ln, Zn)**.

3b-(Sm, Zn): ¹H NMR (600 MHz, CD₃CN) δ 8.33 (s, 1H), 7.52 (d, *J* = 2.0 Hz, 1H), 7.39 (d, *J* = 7.6 Hz, 1H), 7.34 (d, *J* = 2.0 Hz, 1H), 7.15 (d, *J* = 7.6 Hz, 1H), 6.99 (s, 1H), 6.82 (d, *J* = 7.6 Hz, 1H), 5.61 (d, *J* = 7.6 Hz, 1H), 4.69 ~ 4.61 (m, 1H), 4.47 (s, 1H), 4.20 (s, 1H), 4.18 (s, 1H), 3.88 (s, 1H), 2.26 (s, 3H). ¹³C NMR (101 MHz, Acetonitrile-*d*₃) δ 177.17, 170.27, 165.09, 152.14, 144.20, 143.69, 141.38, 131.44, 130.34, 127.07, 125.18, 123.94, 123.02, 121.23, 65.33, 64.65, 40.11, 19.73. ESI-TOF-MS for **3b-(Sm, Zn)**: the following picked signals are those at the highest intensities. *m/z* calcd. for [3b-(Sm, Zn)(OTf)₂]²⁺ 1190.1810, found 1190.1812; calcd. for [3b-(Sm, Zn)(OTf)₁]³⁺ 743.8032, found 743.8033; calcd. for [3b-(Sm, Zn)]⁴⁺ 520.6143, found 520.6147.

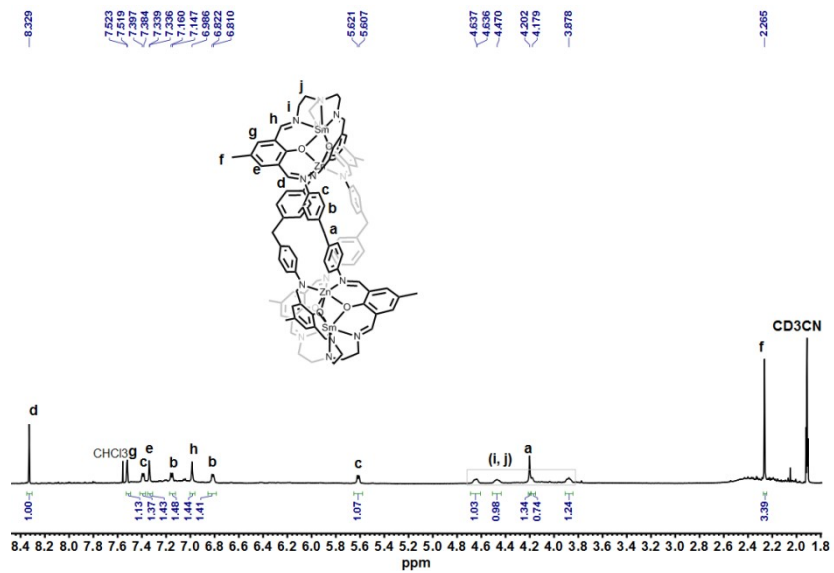


Figure S18. ¹H NMR spectrum of 3b-(Sm, Zn) (600 MHz, CD₃CN, 298 K).

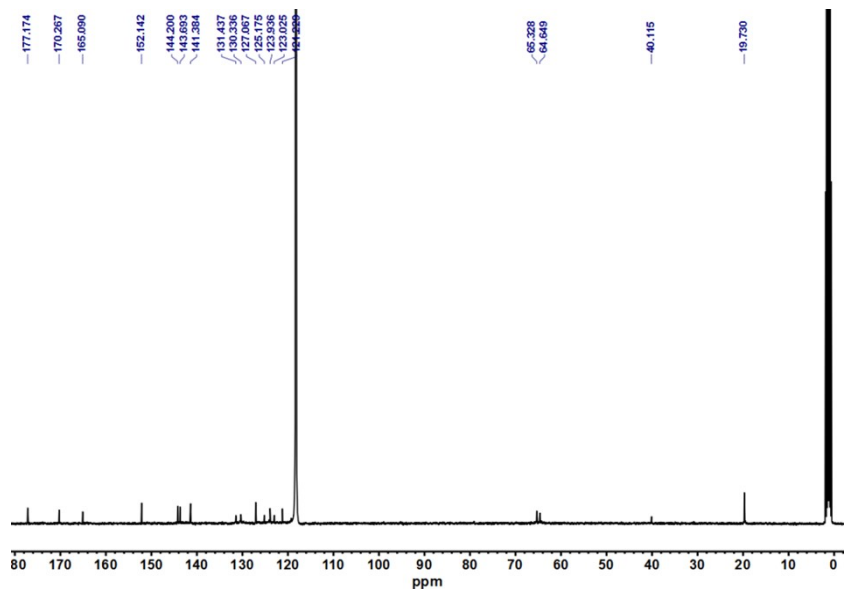


Figure S19. ¹³C NMR spectrum of 3b-(Sm, Zn) (101 MHz, CD₃CN, 298 K).

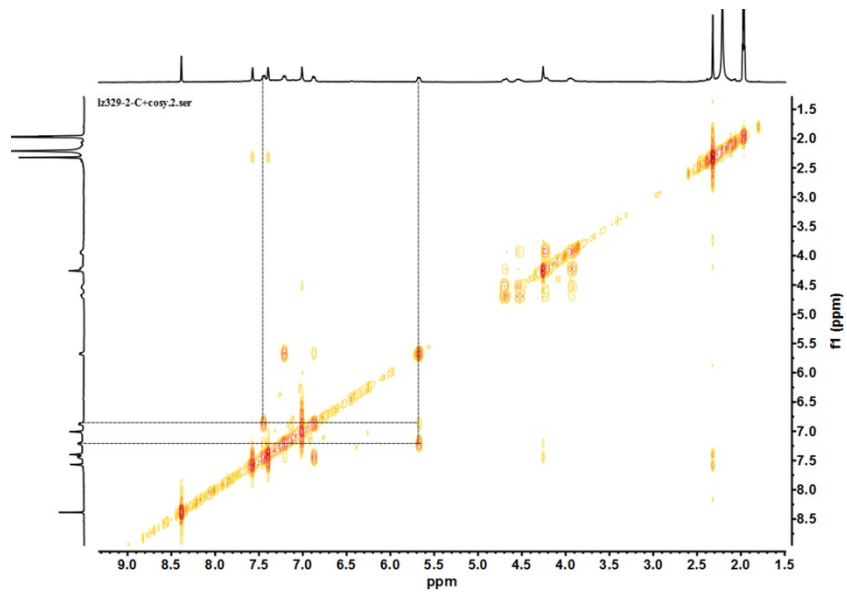


Figure S20. ¹H-¹H COSY NMR spectrum of 3b-(Sm, Zn) (400 MHz, CD₃CN, 298 K).

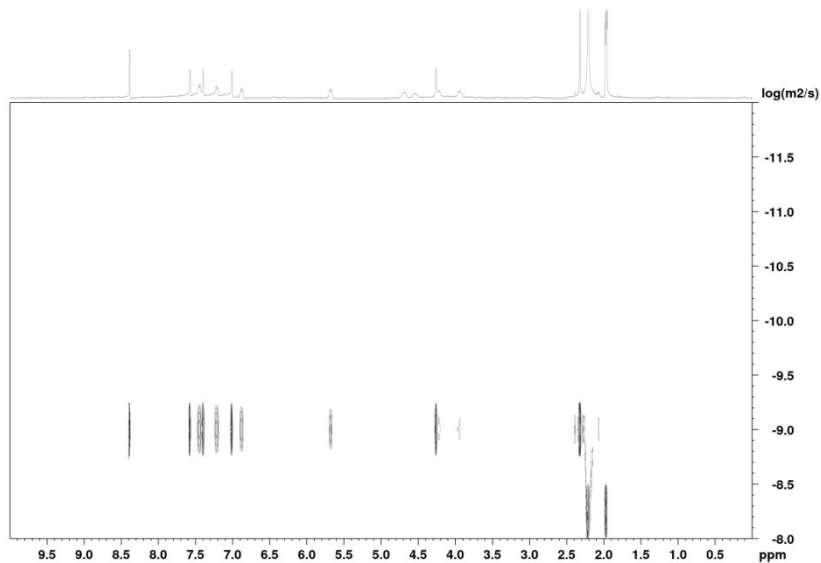


Figure S21. ¹H DOSY NMR spectrum of 3b-(Sm, Zn) (400 MHz, CD₃CN, 298 K).

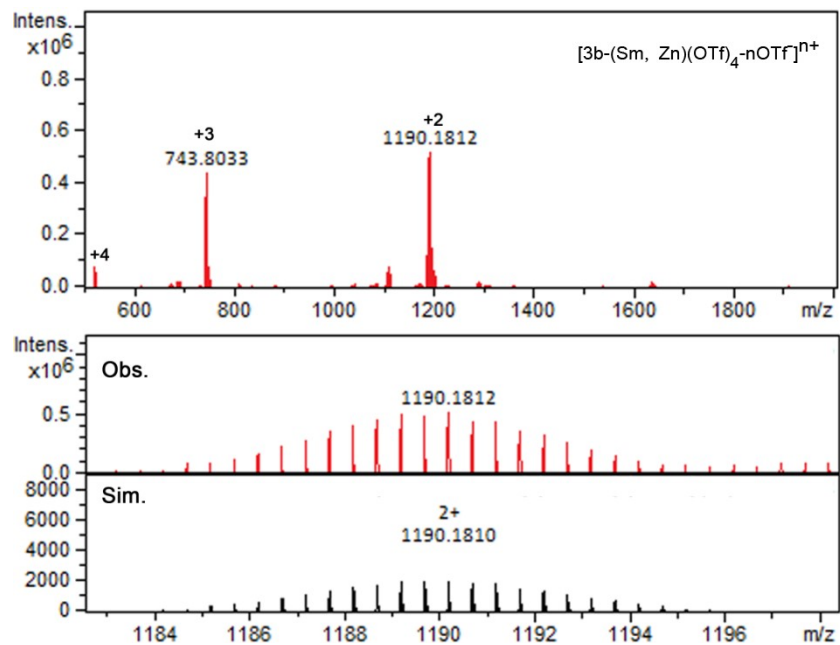


Figure S22. ESI-TOF-MS spectrum of **3b-(Sm, Zn)** with insets showing the observed and simulated isotopic patterns of the +2 peak.

3b-(Eu, Zn): ESI-TOF-MS for **3b-(Eu, Zn)**: the following picked signals are those at the highest intensities. m/z calcd. for $[3b-(Eu, Zn)(OTf)_2]^{2+}$ 1191.1828, found 1191.1833; calcd. for $[3b-(Eu, Zn)(OTf)_1]^{3+}$ 744.4710, found 744.4714.

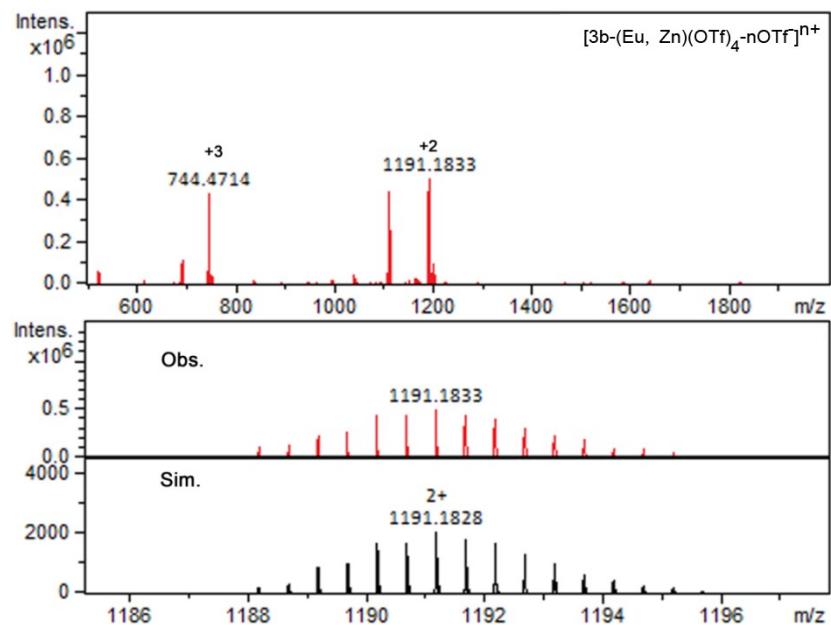


Figure S23. ESI-TOF-MS spectrum of **3b-(Eu, Zn)** with insets showing the observed and simulated isotopic patterns of the +2 peak.

3b-(Yb, Zn): ESI-TOF-MS for **3b-(Yb, Zn)**: the following picked signals are those at the highest intensities. m/z calcd. for $[3b-(Yb, Zn)(OTf)_2]^{2+}$ 1212.2005, found 1212.1999; calcd. for $[3b-(Yb, Zn)(OTf)_1]^{3+}$ 758.4829, found 758.4825.

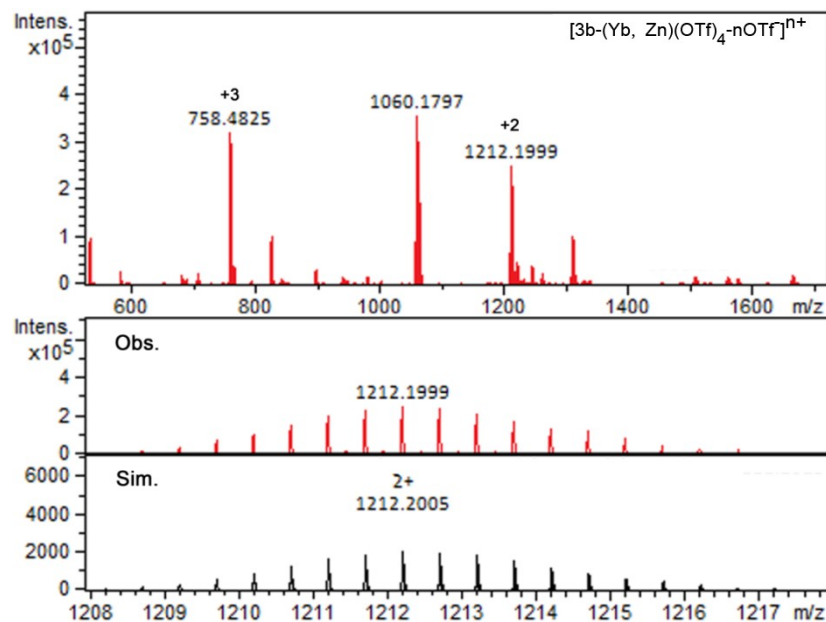


Figure S24. ESI-TOF-MS spectrum of **3b-(Yb, Zn)** with insets showing the observed and simulated isotopic patterns of the +2 peak.

3b-(Lu, Zn): ESI-TOF-MS for **3b-(Lu, Zn)**: the following picked signals are those at the highest intensities. m/z calcd. for $[3b-(Lu, Zn)(OTf)_2]^{2+}$ 1214.2030, found 1214.2024; calcd. for $[3b-(Lu, Zn)(OTf)_1]^{3+}$ 759.8178, found 759.8176.

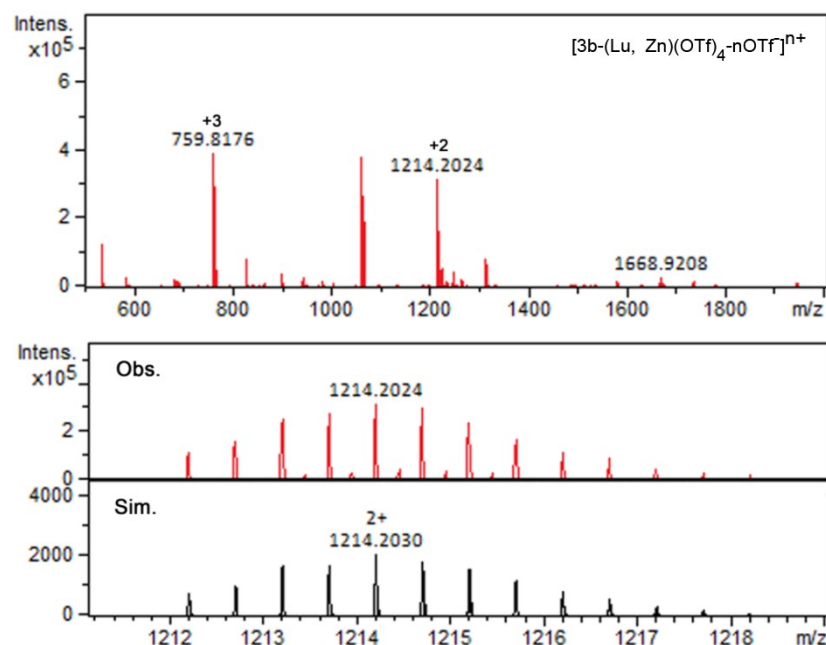


Figure S25. ESI-TOF-MS spectrum of **3b-(Lu, Zn)** with insets showing the observed and simulated isotopic patterns of the +2 peak.

3b-(Gd, Zn): ESI-TOF-MS for **3b-(Gd, Zn)**: the following picked signals are those at the highest intensities. m/z calcd. for $[3b-(Gd, Zn)(OTf)_2]^{2+}$ 1196.19, found 1191.19; calcd. for $[3b-(Gd, Zn)(OTf)_1]^{3+}$ 747.81, found 747.81; calcd. for $[3b-(Gd, Zn)(OTf)_1]^{4+}$ 523.62, found 523.62.

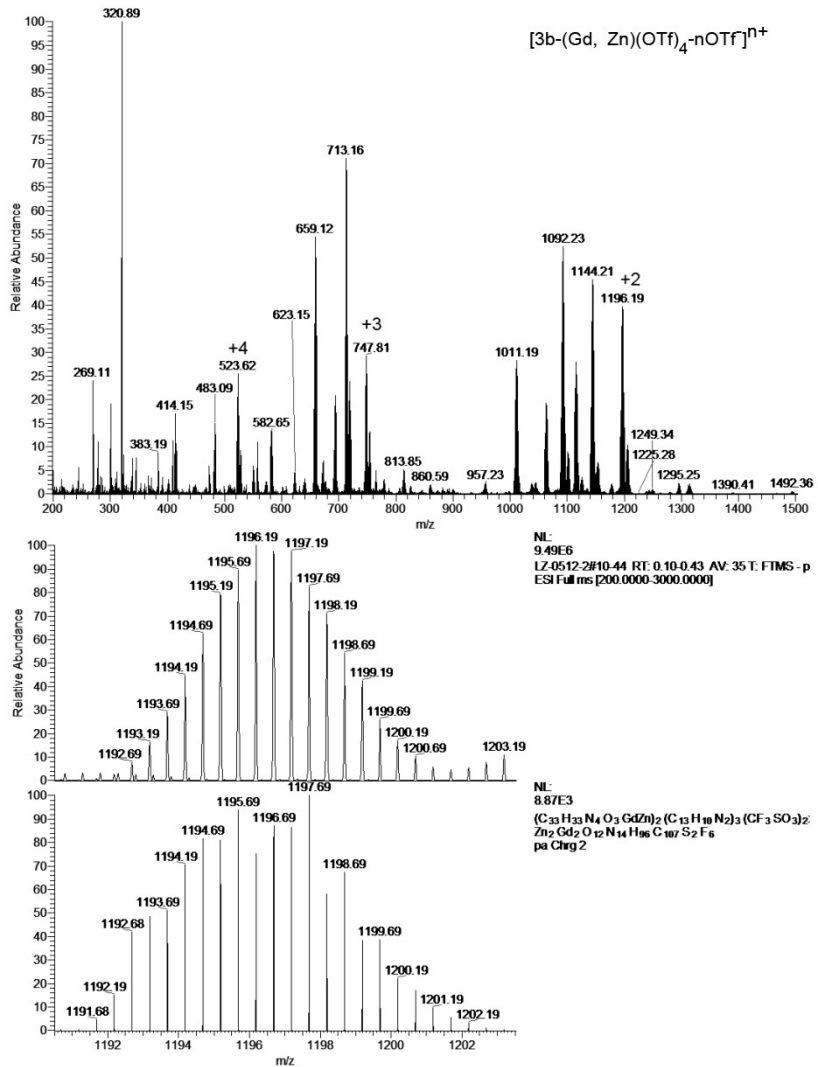


Figure S26. ESI-TOF-MS spectrum of **3b-(Gd, Zn)** with insets showing the observed and simulated isotopic patterns of the +2 peak.

3c-(Sm, Zn): 1H NMR (600 MHz, CD₃CN) δ 8.39 (s, 1H), 7.49 (d, J = 2.0 Hz, 1H), 7.48 – 7.45 (m, 1H), 7.32 (d, J = 2.0 Hz, 1H), 7.03 (dd, J = 8.4, 2.4 Hz, 1H), 6.98 (s, 1H), 6.94 (d, J = 8.8 Hz, 1H), 6.75 (d, J = 8.8 Hz, 1H), 6.72 (dd, J = 8.4, 2.4 Hz, 1H), 5.79 (dd, J = 8.4, 2.4 Hz, 1H), 4.65 (d, J = 12.6 Hz, 1H), 4.44 (s, 1H), 4.21 (d, J = 12.6 Hz, 1H), 3.90 (s, 1H), 2.23 (s, 3H). ESI-TOF-MS for **3c-(Sm, Zn)**: the following picked signals are those at the highest intensities. m/z calcd. for $[3c-(Sm, Zn)(OTf)_2]^{2+}$ 1196.19, found 1191.19; calcd. for $[3c-(Sm, Zn)(OTf)_1]^{3+}$ 747.81, found 747.81; calcd. for $[3c-(Sm, Zn)(OTf)_1]^{4+}$ 523.62, found 523.62.

$\text{Zn}(\text{OTf})_2]^{2+}$ 1328.2373, found 1328.2371; calcd. for $[\text{3c-(Sm, Zn)}(\text{OTf})_1]^{3+}$ 835.8407, found 835.8412; calcd. for $[\text{3c-(Sm, Zn)}]^{4+}$ 589.6425, found 589.6431.

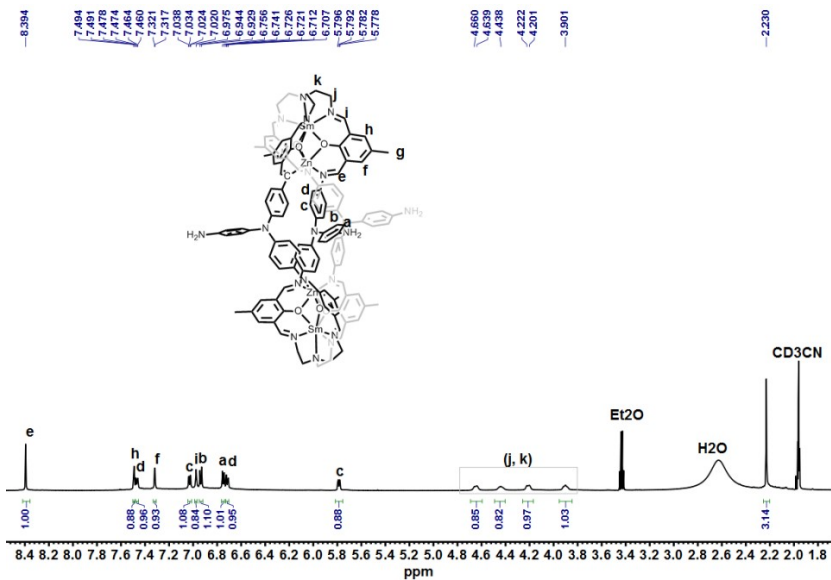


Figure S27. ^1H NMR spectrum of $[\text{3c-(Sm, Zn)}]$, (600 MHz, CD_3CN , 298 K).

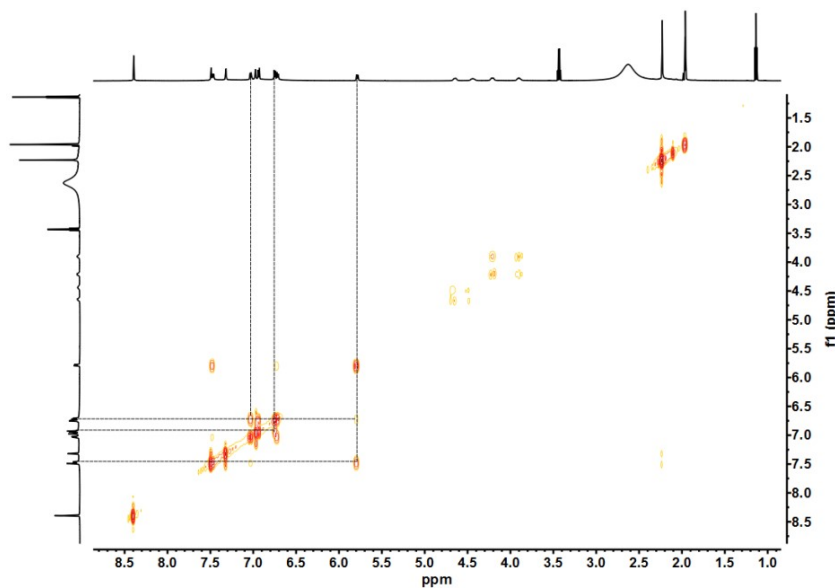


Figure S28. ^1H - ^1H COSY NMR spectrum of $[\text{3c-(Sm, Zn)}]$ (400 MHz, CD_3CN , 298 K).

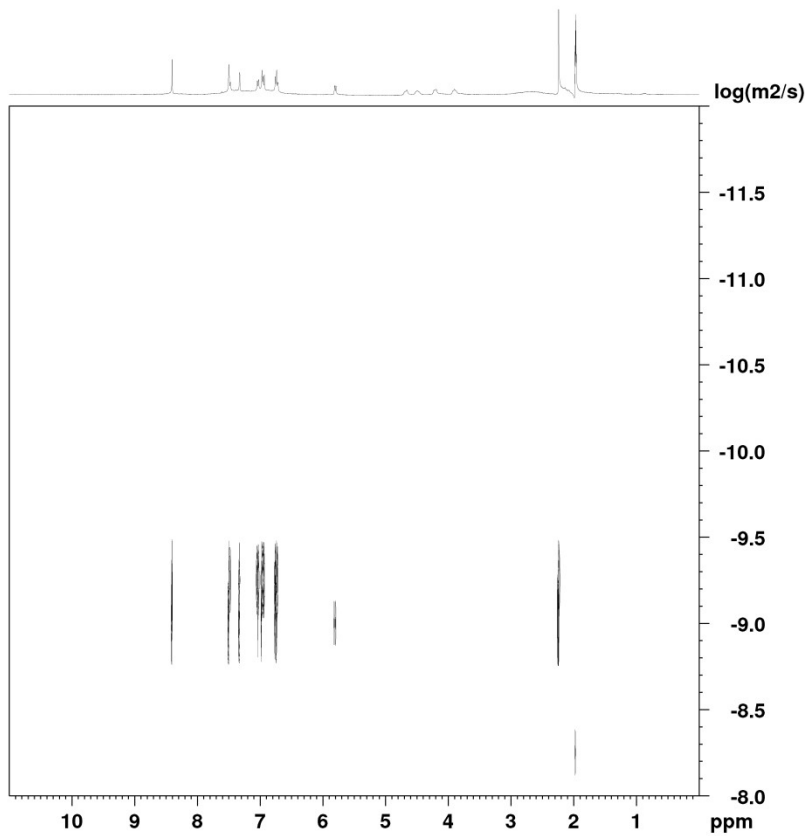


Figure S29. ¹H DOSY NMR spectrum of **3c-(Sm, Zn)** (400 MHz, CD₃CN, 298 K).

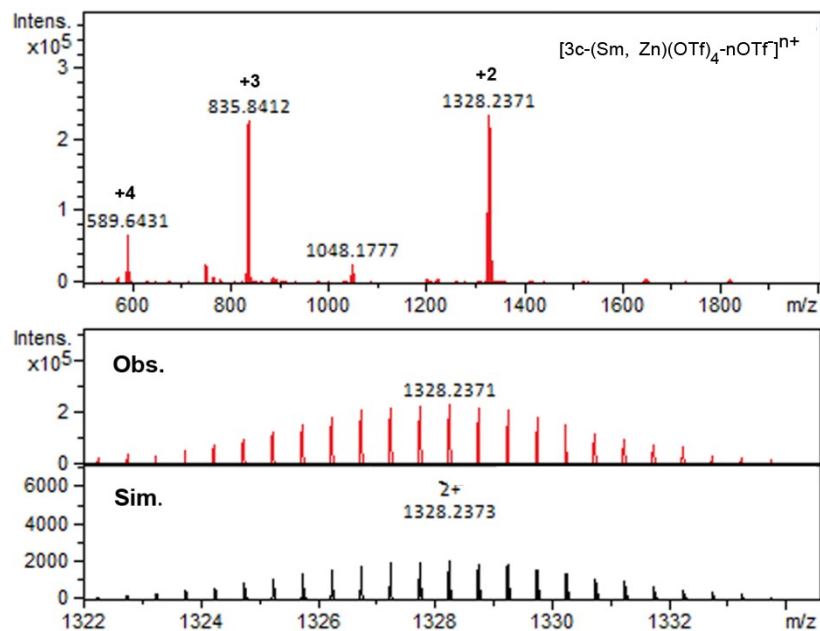


Figure S30. ESI-TOF-MS spectrum of **3c-(Sm, Zn)** with insets showing the observed and simulated isotopic patterns of the +2 peak.

3c-(Eu, Zn): ESI-TOF-MS for **3c-(Eu, Zn):** the following picked signals are those at the highest intensities. *m/z* calcd. for [3c-(Eu, Zn)(OTf)₂]²⁺ 1329.2393, found

1329.2392; calcd. for $[3\text{c-(Eu, Zn)}(\text{OTf})_1]^{3+}$ 836.5087, found 836.5095; calcd. for $[3\text{c-(Eu, Zn)}]^{4+}$ 590.1434, found 590.1440.

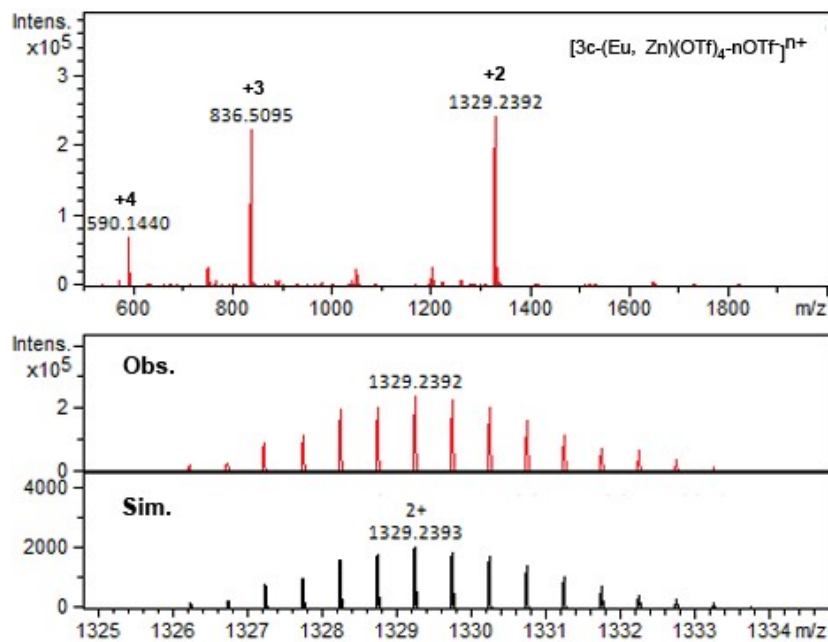


Figure S31. ESI-TOF-MS spectrum of **3c-(Eu, Zn)** with insets showing the observed and simulated isotopic patterns of the $+2$ peak.

3c-(Yb, Zn): ESI-TOF-MS for **3c-(Yb, Zn)**: the following picked signals are those at the highest intensities. m/z calcd. for $[3\text{c-(Yb, Zn)}(\text{OTf})_2]^{2+}$ 1350.2569, found 1350.2562; calcd. for $[3\text{c-(Yb, Zn)}(\text{OTf})_1]^{3+}$ 850.5204, found 850.5206; calcd. for $[3\text{c-(Yb, Zn)}]^{4+}$ 600.6522, found 600.6521.

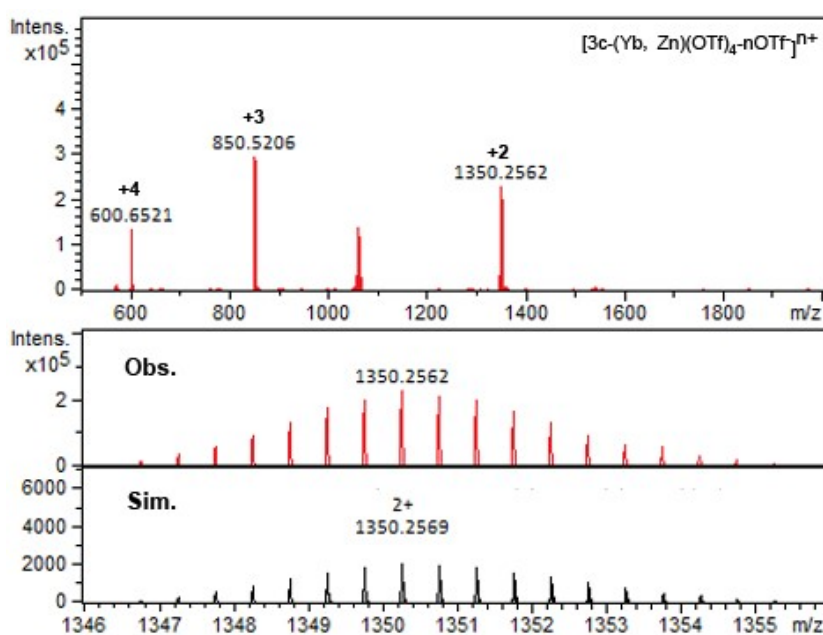


Figure S32. ESI-TOF-MS spectrum of **3c-(Yb, Zn)** with insets showing the observed and simulated isotopic patterns of the +2 peak.

3c-(Lu, Zn): ^1H NMR (400 MHz, CD_3CN) δ 8.44 (s, 1H), 8.10 (s, 1H), 7.55 (s, 1H), 7.51 (s, 1H), 7.15 (d, $J = 8.0$ Hz, 1H), 6.80 (d, $J = 8.0$ Hz, 1H), 6.77 (d, 1H), 6.62 (d, $J = 8.0$ Hz, 1H), 6.22 (d, $J = 8.0$ Hz, 1H), 5.34 (d, $J = 8.0$ Hz, 1H), 4.18 (s, 1H), 3.98 (s, 1H), 3.85 (s, 1H), 3.39 (s, 1H), 3.04 (s, 1H), 2.32 (s, 3H). ESI-TOF-MS for **3c-(Lu, Zn)**: the following picked signals are those at the highest intensities. m/z calcd. for $[\mathbf{3c-(Lu, Zn)(OTf)}_2]^{2+}$ 1352.2595, found 1352.2591; calcd. for $[\mathbf{3c-(Lu, Zn)(OTf)}_1]^{3+}$ 851.8555, found 851.8557; calcd. for $[\mathbf{3c-(Lu, Zn)}]^{4+}$ 601.6535, found 601.6538.

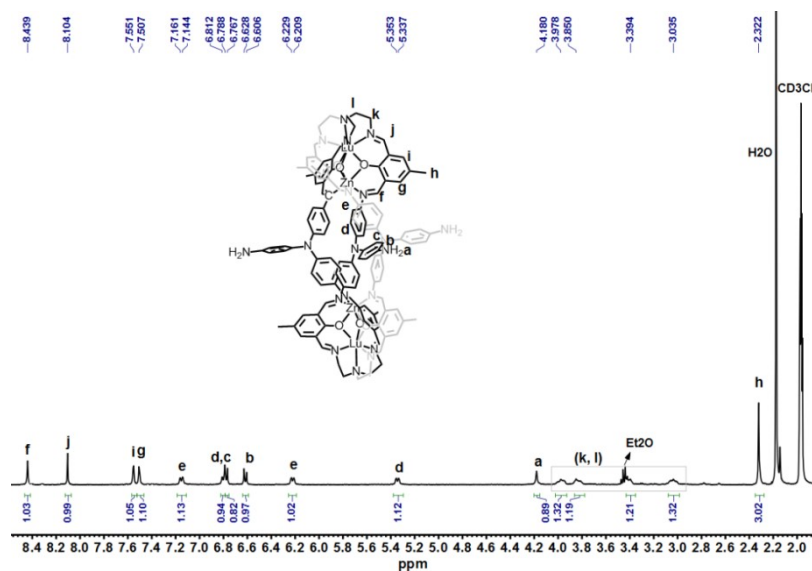


Figure S33. ^1H NMR spectrum of **3c-(Lu, Zn)** (400 MHz, CD_3CN , 298 K).

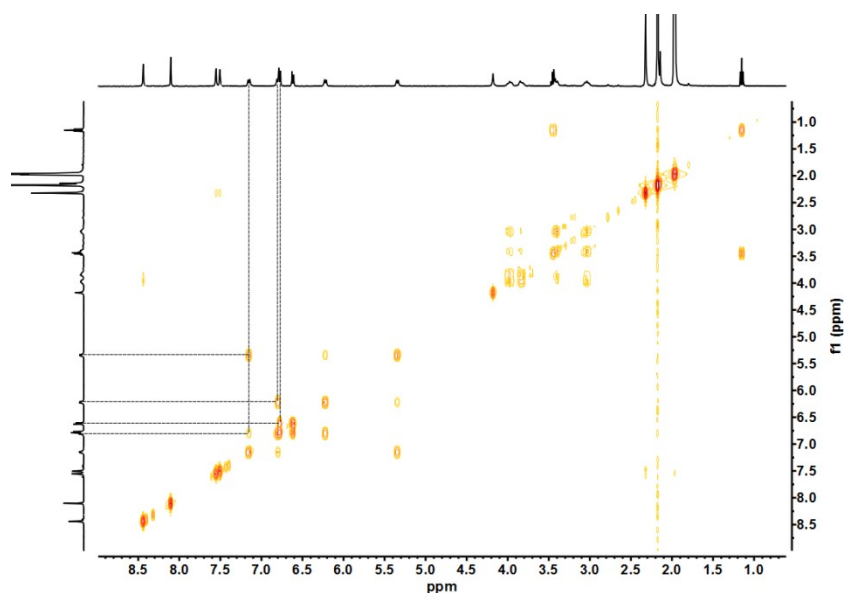


Figure S34. ^1H - ^1H COSY NMR spectrum of **3c-(Lu, Zn)** (400 MHz, CD_3CN , 298 K).

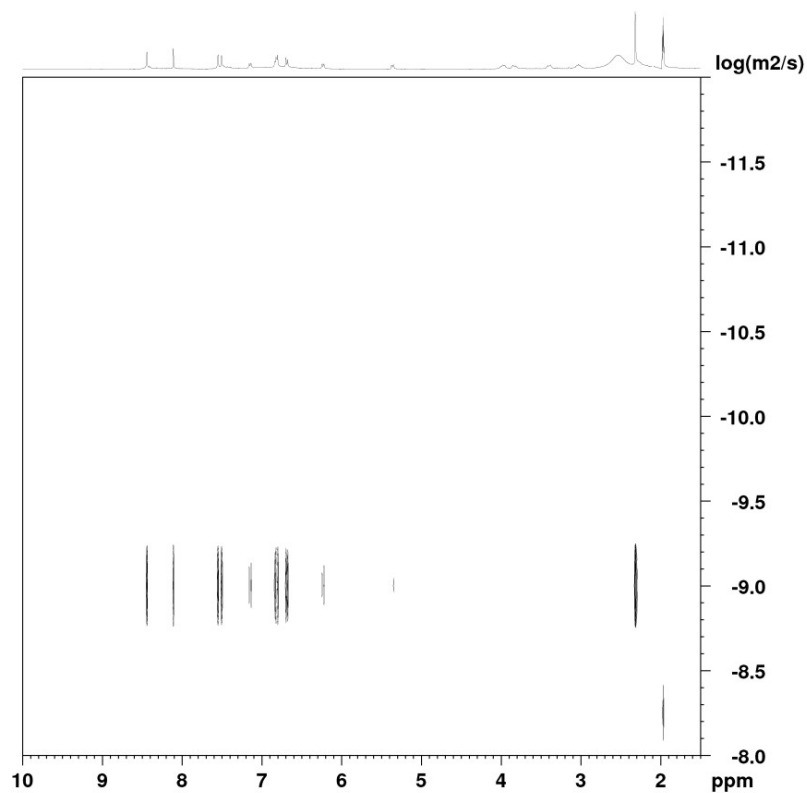


Figure S35. ^1H DOSY NMR spectrum of **3c-(Lu, Zn)** (400 MHz, CD_3CN , 298 K).

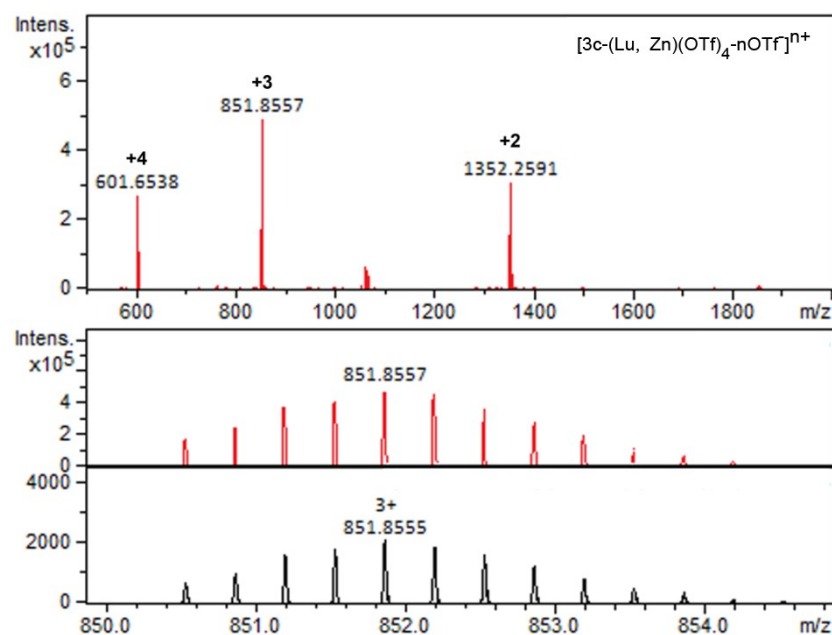


Figure S36. ESI-TOF-MS spectrum of **3c-(Lu, Zn)** with insets showing the observed and simulated isotopic patterns of the +3 peak.

3c-(Gd, Zn): ESI-TOF-MS for **3c-(Gd, Zn)**: the following picked signals are those at the highest intensities. m/z calcd. for $[3c\text{-(Gd, Zn)}(\text{OTf})_2]^{2+}$ 1334.74, found 1334.74; calcd. for $[3c\text{-(Gd, Zn)}(\text{OTf})_1]^{3+}$ 839.84, found 839.84; calcd. for $[3c\text{-(Gd, Zn)}]^{4+}$ 592.65, found 592.65.

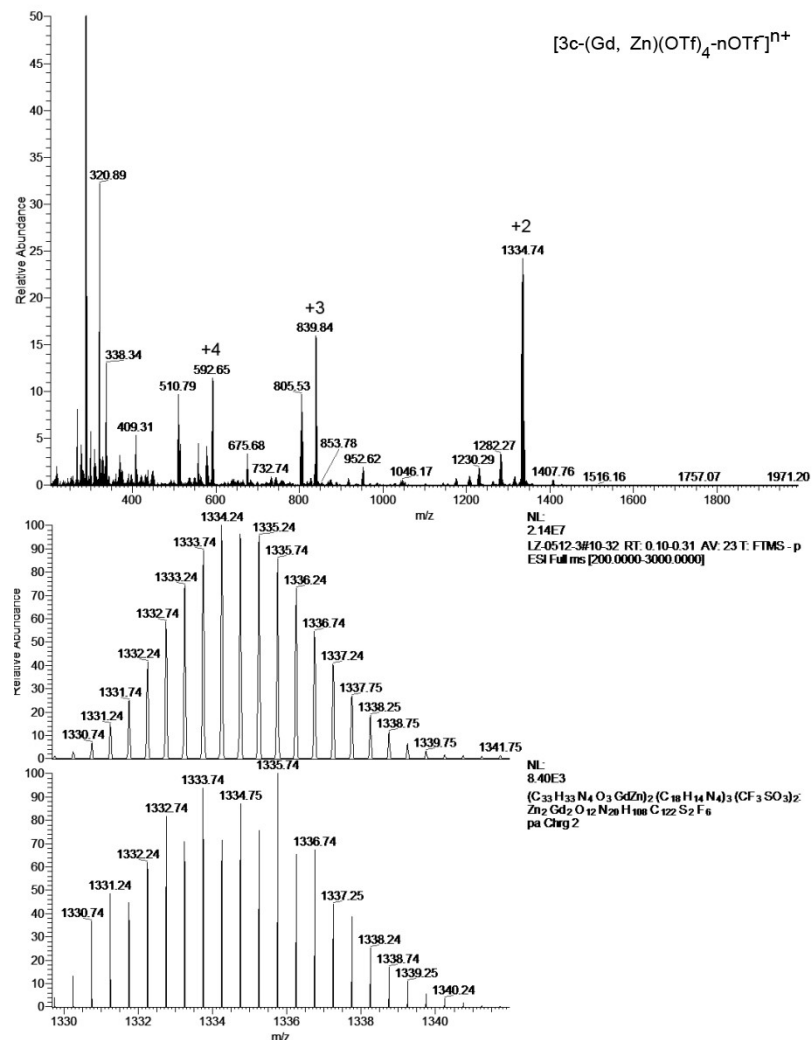


Figure S37. ESI-TOF-MS spectrum of **3c-(Gd, Zn)** with insets showing the observed and simulated isotopic patterns of the +2 peak.

4. UV-Vis and FL spectrum

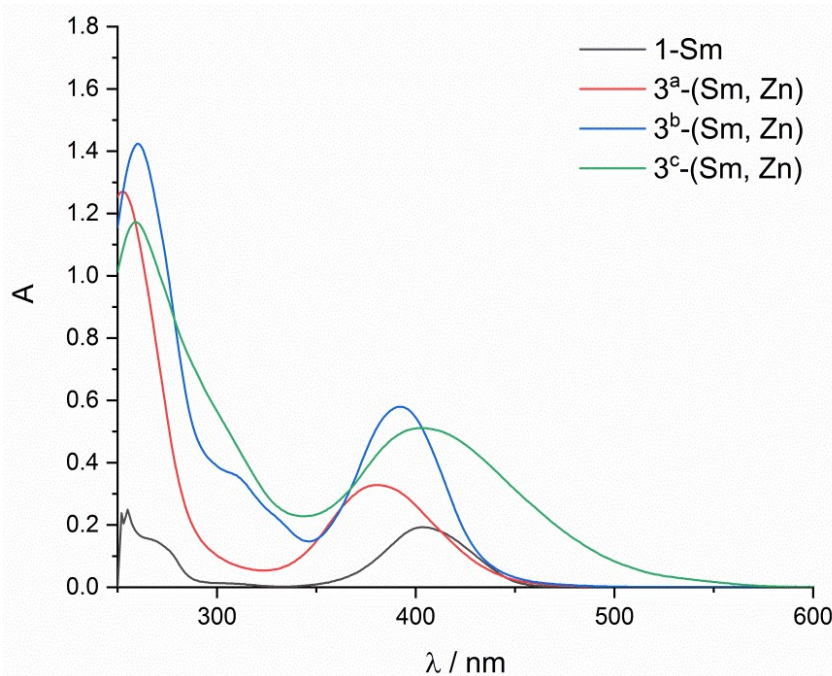


Figure S38. UV-Vis absorption spectra of **1-Sm** (1.0×10^{-5} M in MeCN), **3a-(Sm, Zn)** (1.0×10^{-5} M in MeCN), **3b-(Sm, Zn)** (1.0×10^{-5} M in MeCN), **3c-(Sm, Zn)** (1.0×10^{-5} M in MeCN) at 298 K.

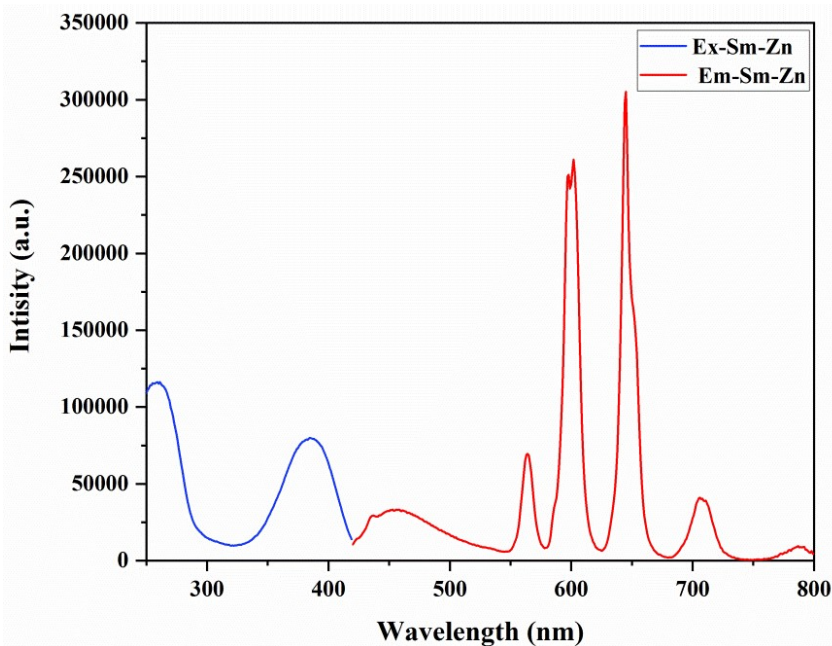


Figure S39. Excitation (blue line) and emission (red line, for the visible region only) of **3a-(Sm, Zn)**. (1.0×10^{-5} M; $\lambda_{\text{ex}} = 386$ nm, $\lambda_{\text{em}} = 645$ nm, slits = 3-4).

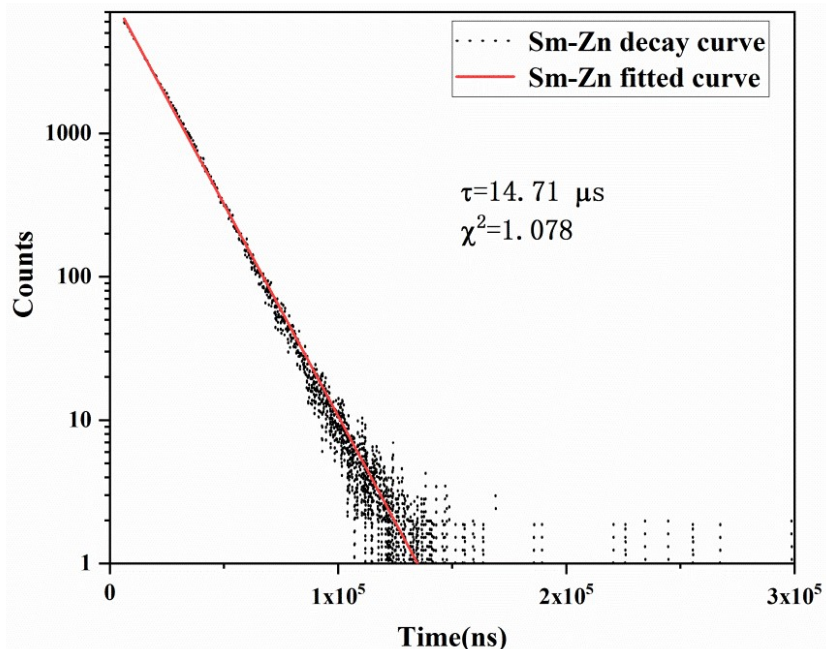


Figure S40. Excited state decay curve (black dots) with mono exponential fit (red line) of **3a-(Sm, Zn)**. (1.0×10^{-5} M in MeCN; $\lambda_{\text{ex}} = 386$ nm, $\lambda_{\text{em}} = 645$ nm; lifetime = 14.71 μs).

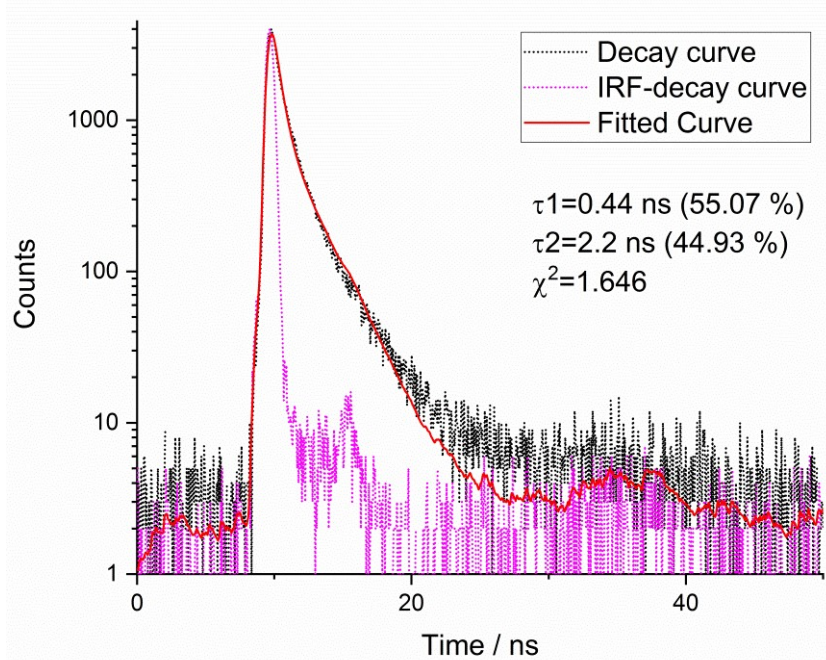


Figure S41. Luminescent lifetime of organic backbone of **3a-(Sm, Zn)** measured at 456 nm (1.0×10^{-5} M in MeCN; lifetime = 1.26 ns).

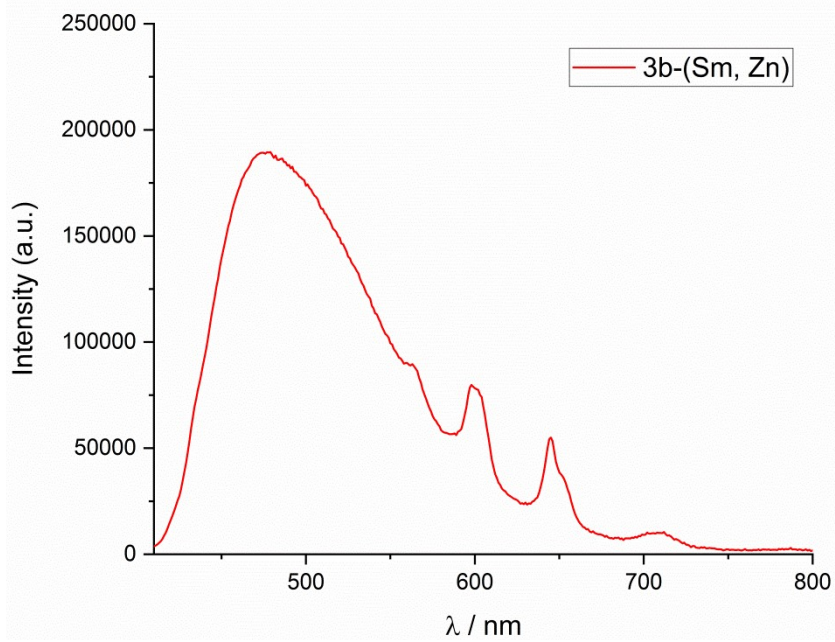


Figure S42. Emission (for the visible region only) of **3b-(Sm, Zn)**. (1.0×10^{-5} M in MeCN; $\lambda_{\text{ex}} = 386$ nm, $\lambda_{\text{em}} = 645$ nm, slits = 4-4).

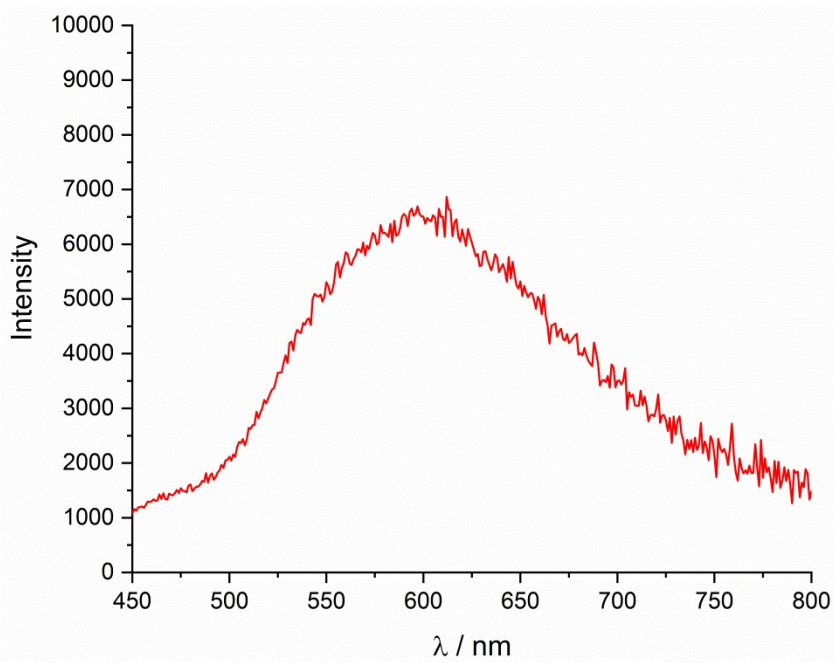


Figure S43. Emission (for the visible region only) of **3c-(Sm, Zn)**. (1.0×10^{-5} M in MeCN; $\lambda_{\text{ex}} = 386$ nm, $\lambda_{\text{em}} = 645$ nm).

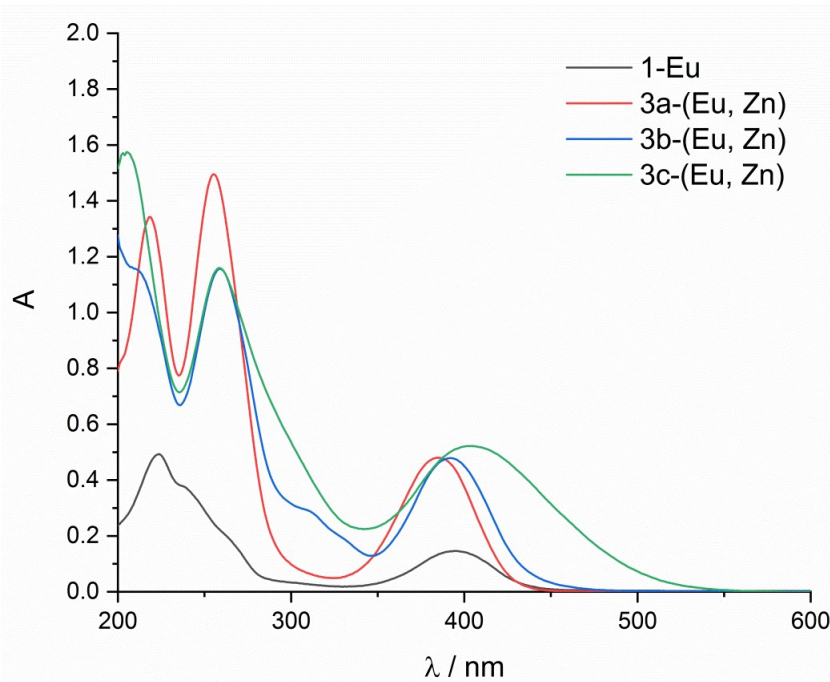


Figure S44. UV-Vis absorption spectra of **1-Eu**, (1.0×10^{-5} M in MeCN), **3a-(Eu, Zn)** (1.0×10^{-5} M in MeCN), **3b-(Eu, Zn)** (1.0×10^{-5} M in MeCN), **3c-(Eu, Zn)** (1.0×10^{-5} M in MeCN) at 298 K.

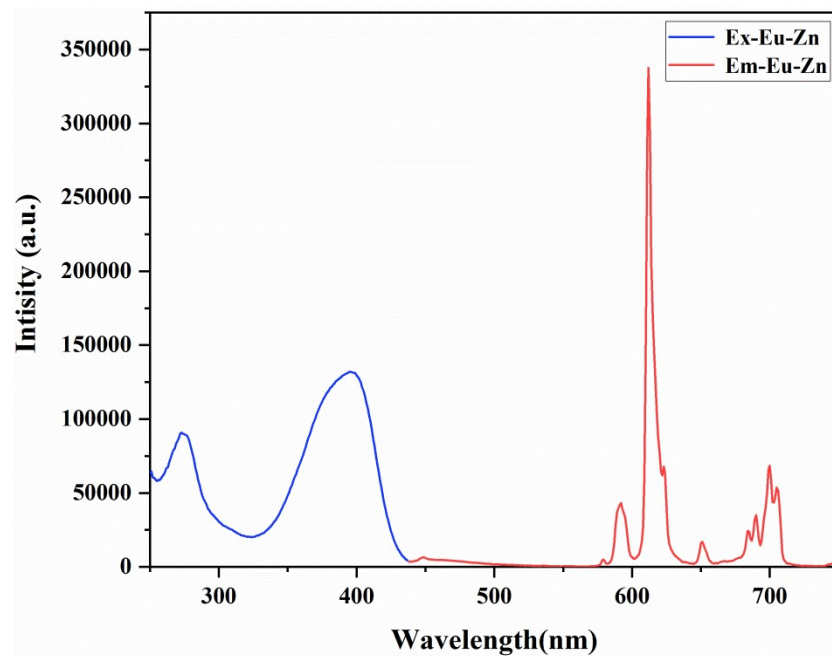


Figure S45. Excitation (blue line) and emission (red line) of **3a-(Eu, Zn)**. (1.0×10^{-5} M in MeCN; $\lambda_{\text{ex}} = 393$ nm, $\lambda_{\text{em}} = 612$ nm).

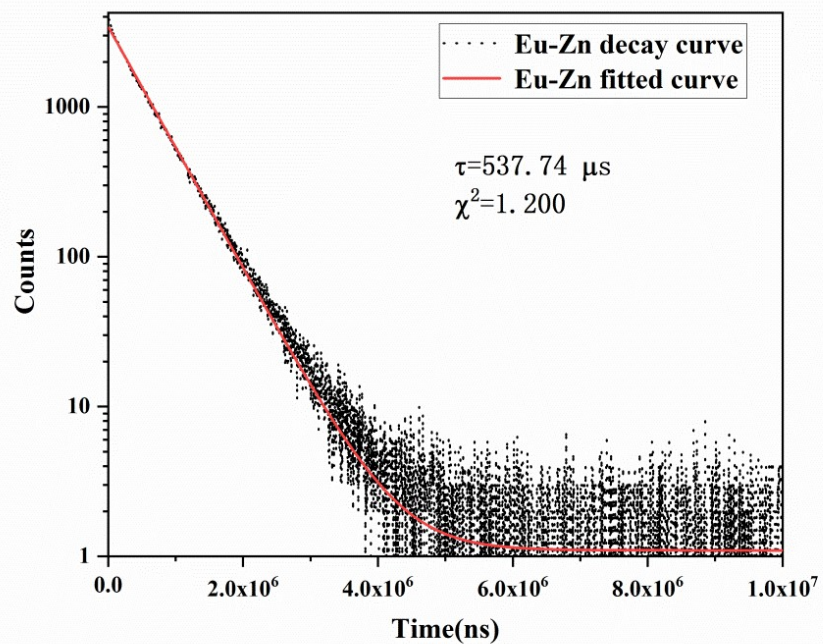


Figure S46. Excited state decay curve (black dots) with mono exponential fit (red line) of **3a-(Eu, Zn)**. (1.0×10^{-5} M in MeCN; $\lambda_{\text{ex}} = 393$ nm, $\lambda_{\text{em}} = 612$ nm; lifetime = 14.71 μs).

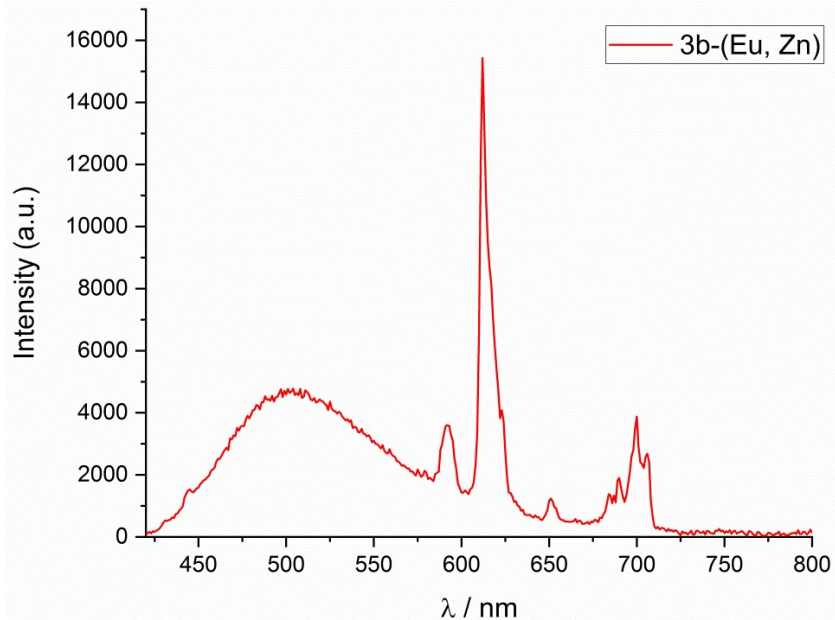


Figure S47. Emission spectrum of **3b-(Eu, Zn)**. (1.0×10^{-5} M in MeCN; $\lambda_{\text{ex}} = 393$ nm, $\lambda_{\text{em}} = 612$ nm, slits = 2-2).

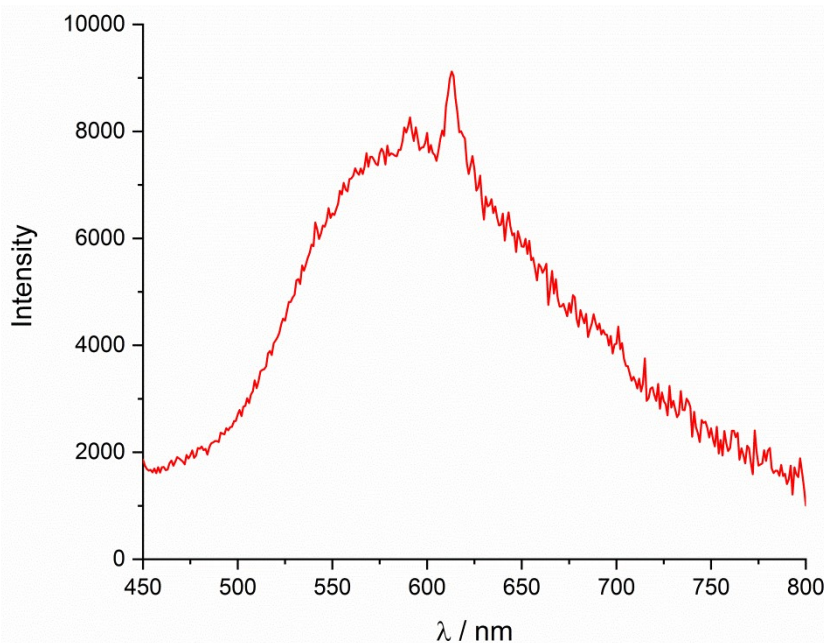


Figure S48. Emission spectrum of **3c-(Eu, Zn)**. (1.0×10^{-5} M in MeCN; $\lambda_{\text{ex}} = 393$ nm, $\lambda_{\text{em}} = 612$ nm).

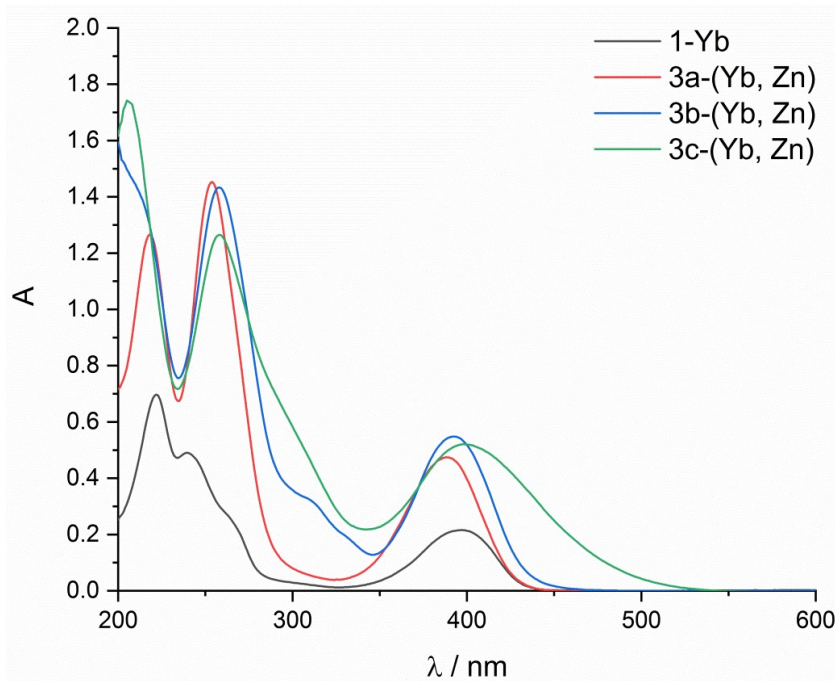


Figure S49. UV-Vis absorption spectra of **1-Yb** (1.0×10^{-5} M in MeCN), **3a-(Yb, Zn)** (1.0×10^{-5} M in MeCN), **3b-(Yb, Zn)** (1.0×10^{-5} M in MeCN), **3c-(Yb, Zn)** (1.0×10^{-5} M in MeCN) at 298 K.

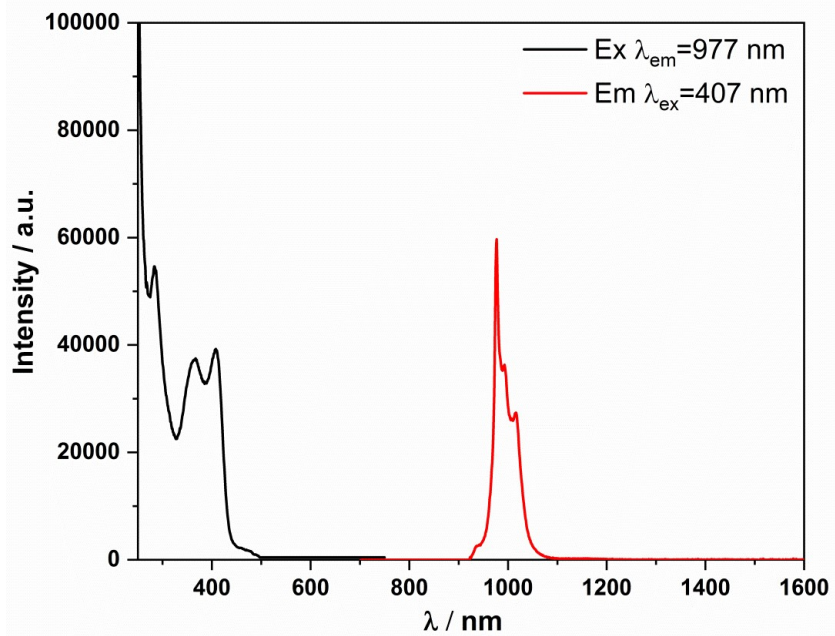


Figure S50. Excitation (black line) and emission (red line) spectra of **3a-(Yb, Zn)**.

(1.0×10^{-5} M in MeCN; $\lambda_{\text{ex}} = 408$ nm, $\lambda_{\text{em}} = 977$ nm).

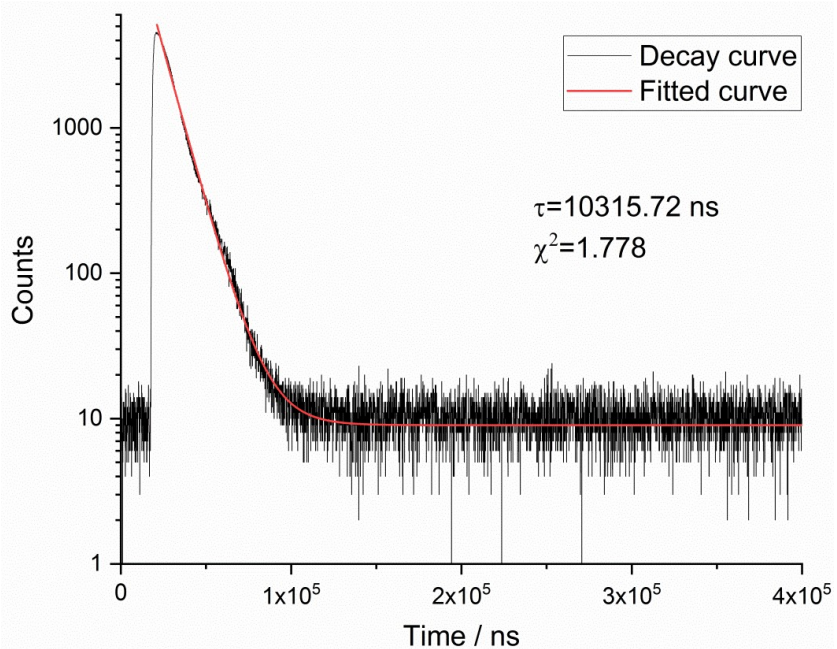


Figure S51. Excited state decay curve (black dots) with mono exponential fit (red line) of **3a-(Yb, Zn)**. (1.0×10^{-5} M in MeCN; $\lambda_{\text{ex}} = 408$ nm, $\lambda_{\text{em}} = 977$ nm; lifetime = 10.32 μ s).

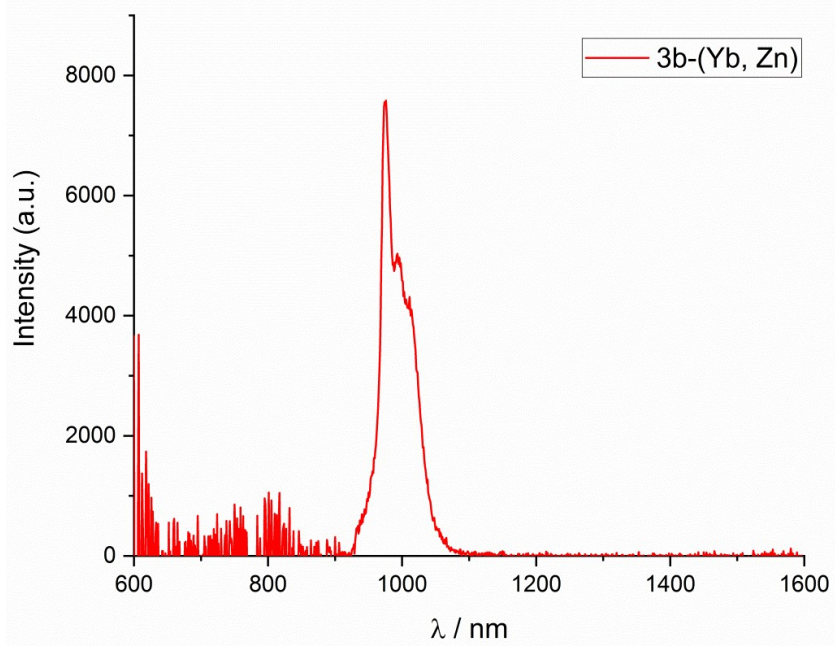


Figure S52. Emission spectrum of **3b-(Yb, Zn)**. (1.0×10^{-5} M in MeCN; $\lambda_{\text{ex}} = 408$ nm, $\lambda_{\text{em}} = 977$ nm).

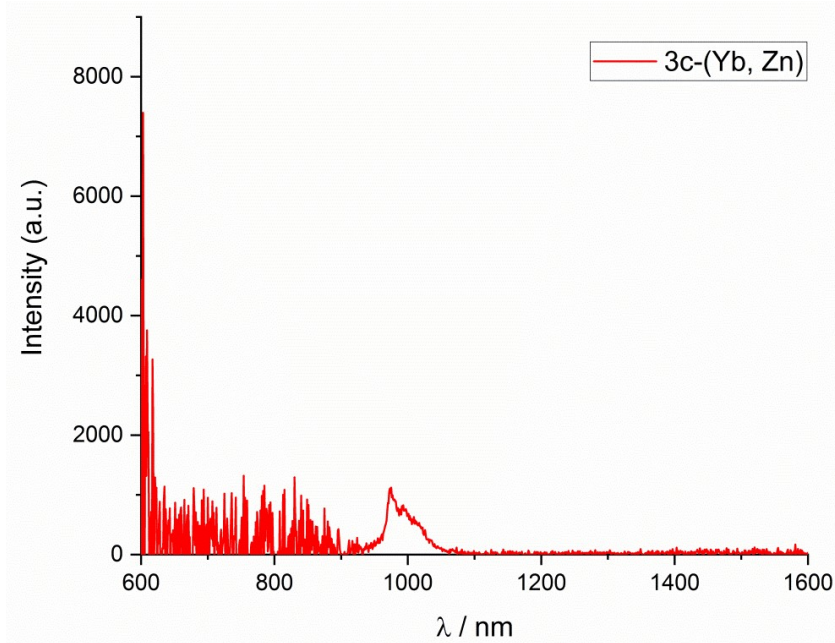


Figure S53. Emission spectrum of **3c-(Yb, Zn)**. (1.0×10^{-5} M in MeCN; $\lambda_{\text{ex}} = 408$ nm, $\lambda_{\text{em}} = 977$ nm).

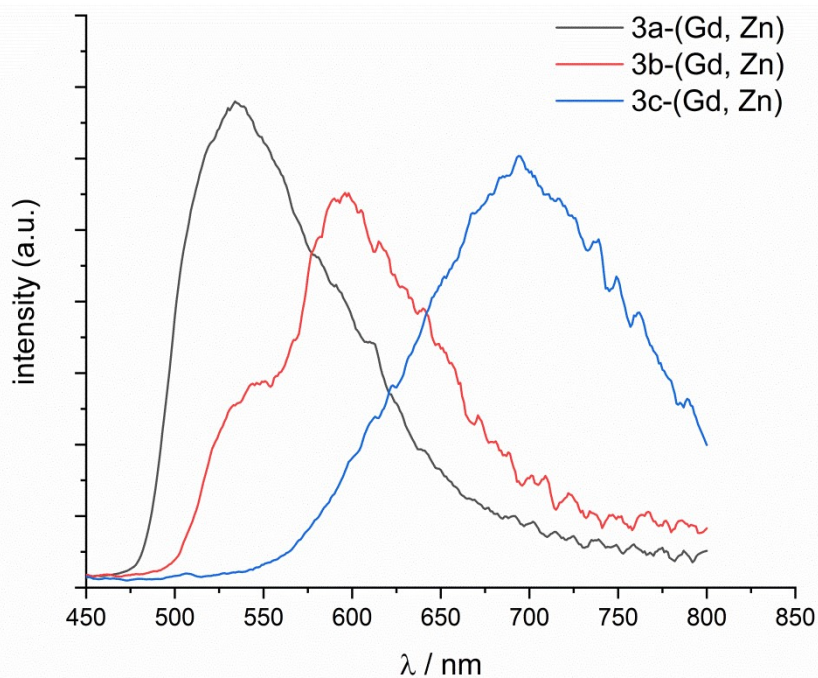


Figure S54. Phosphorescence emission of complexes **3a-3c-(Gd, Zn)** in MeCN at 77 K ($\lambda_{\text{ex}}=390$ nm for **3a-3b-(Gd, Zn)**, $\lambda_{\text{ex}}=414$ nm for **3c-(Gd, Zn)**, $c=1.0 \times 10^{-4}$ M, N_2 , gating = 0.02-10 ms).

5. Magnetic Data

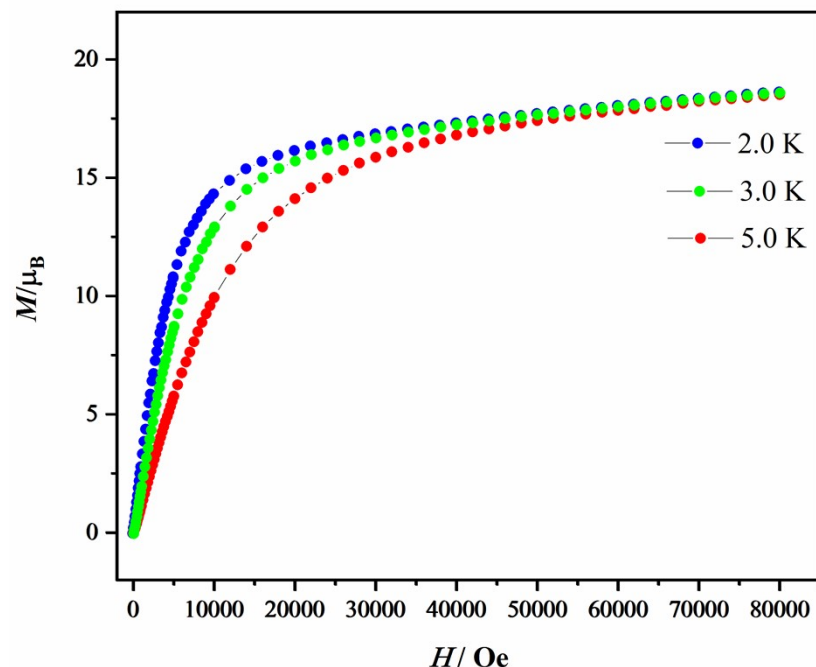


Figure S55. Field-dependent magnetization of **3a'-(Dy, Co)** in the temperature range of 2, 3 and 5 K.

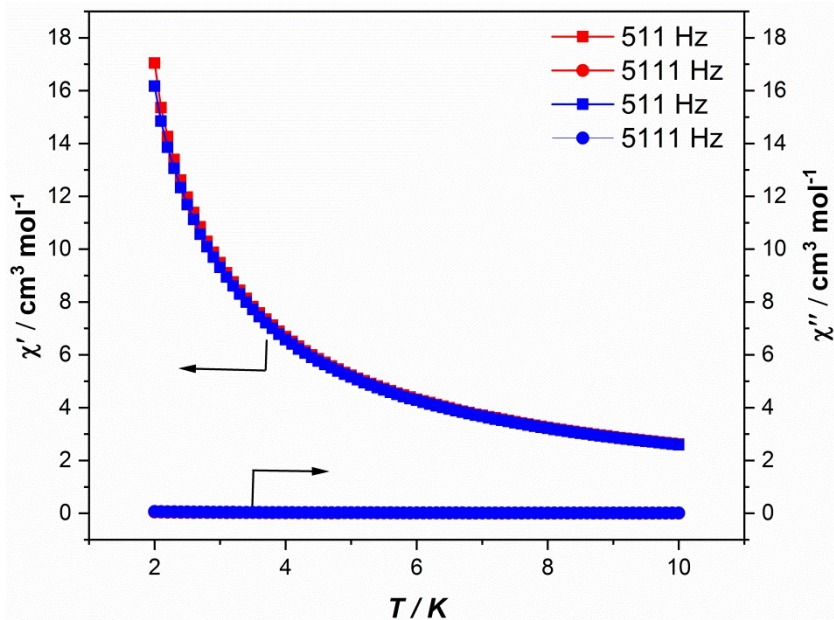


Figure S56. Temperature-dependent in-phase (χ') and out-of-phase (χ'') of **3a'-Dy, Co**) at indicated frequencies under zero dc field.

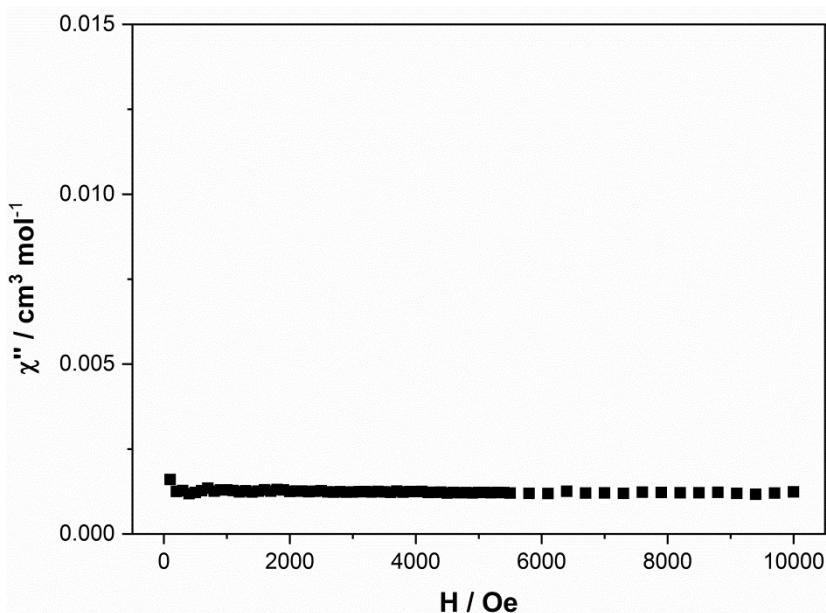


Figure S57. Field dependent χ'' data of **3a'-Dy, Co** in the applied dc field of 0–10000 Oe at 2 K and 1000 Hz.

6. Single crystal X-ray diffraction studies

The X-ray diffraction studies for heterometal-organic macrocycles were carried out on Bruker D8 VENTURE photon II diffractometer with Iμs 3.0 microfocus X-ray source using APEX III program. Data reduction was performed with the saint and SADABS package. The structures were solved by direct methods using SHELXS-97

and refined by full-matrix least-squares on F^2 using SHELXL-2016 program.³ Solvent molecules were highly disordered and could not be reasonably located. These residual intensities were removed by PLATON/SQUEEZE routine⁴. Crystallographic data and other pertinent information for **3a-(Lu, Zn)**, **3b-(Lu, Zn)**, **3c-(Lu, Zn)** and **3a'-(Dy, Co)**, were summarized in Table S1 and Table S2. In **3a-(Lu, Zn)**, some constraints (SIMU, DFIX and SADI) were applied to the free OTf⁻ anions to obtain the chemical-reasonable models and reasonable atomic displacement parameters. In **3b-(Lu, Zn)**, some constraints (SIMU, DFIX, SADI, ISOR and DELU) were applied to the free OTf⁻ anions to obtain the chemical-reasonable models and reasonable atomic displacement parameters. In **3c-(Lu, Zn)**, some constraints (SIMU, EADP and DELU) were applied to obtain the chemical-reasonable models and reasonable atomic displacement parameters. In **3a'-(Dy, Co)**, some constraints (SIMU, DFIX and DELU) were applied to obtain the chemical-reasonable models and reasonable atomic displacement parameters. The CCDC numbers: 2256435 for **3a-(Lu, Zn)**, 2256436 for **3b-(Lu, Zn)**, 2256437 for **3b-(Lu, Zn)** and 2256438 for **3a'-(Dy, Co)**.

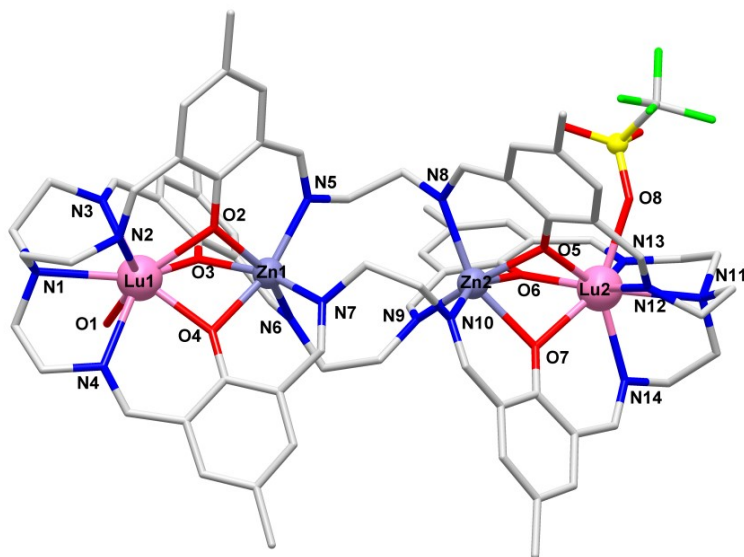


Figure S58. The coordination environment of Lu and Zn in **3a-(Lu, Zn)**.

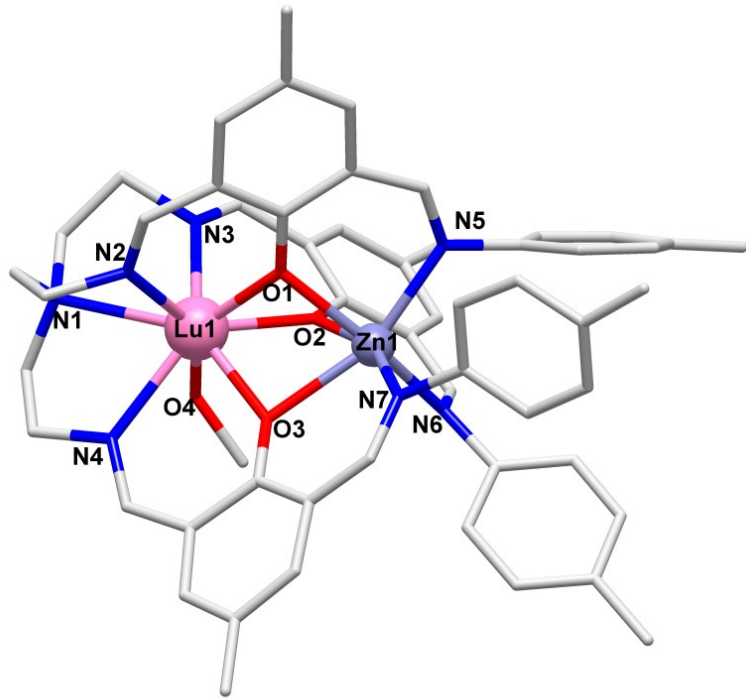


Figure S59. The coordination environment of Lu and Zn in **3b-(Lu, Zn)**.

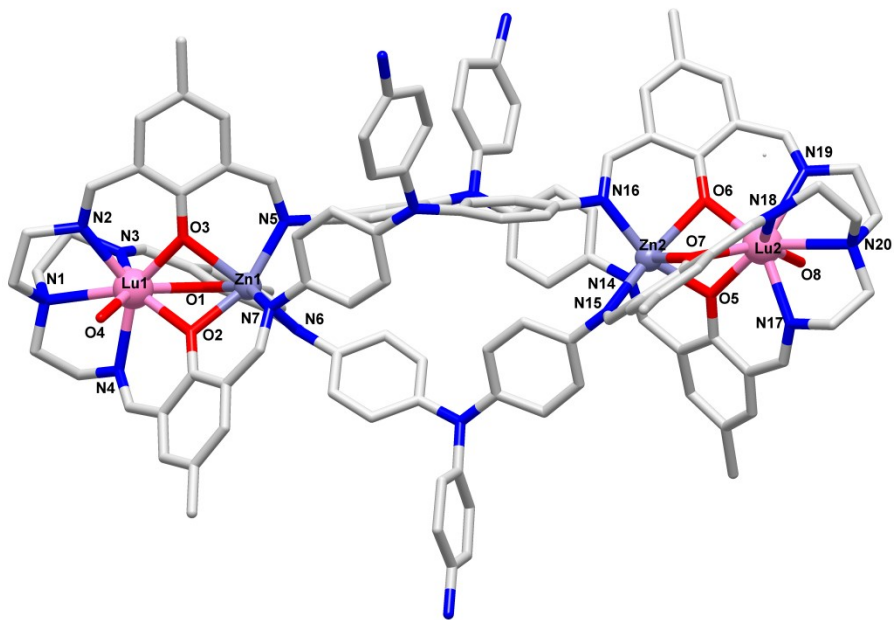


Figure S60. The coordination environment of Lu and Zn in **3c-(Lu, Zn)**.

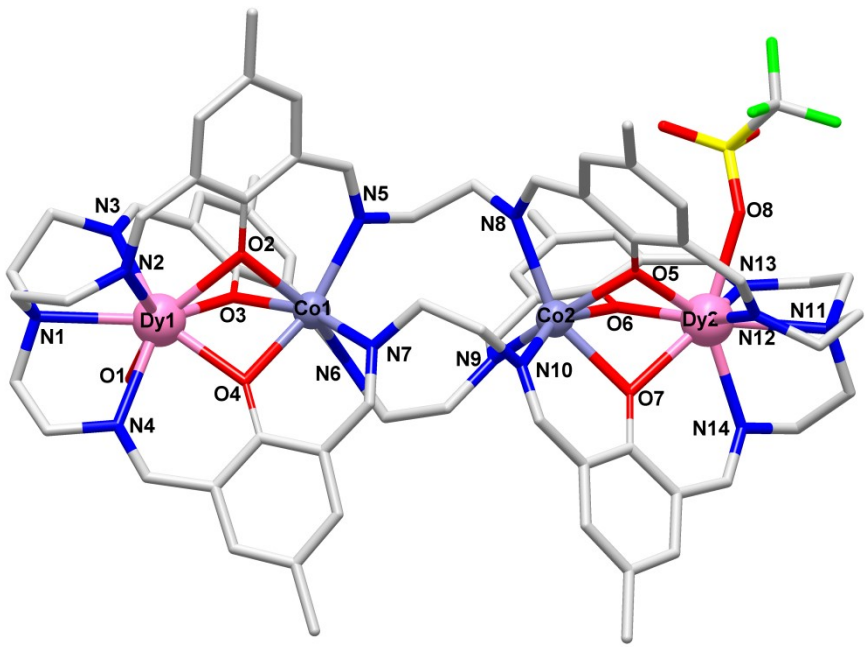


Figure S61. The coordination environment of Dy and Co in **3a'-(Dy, Co)**.

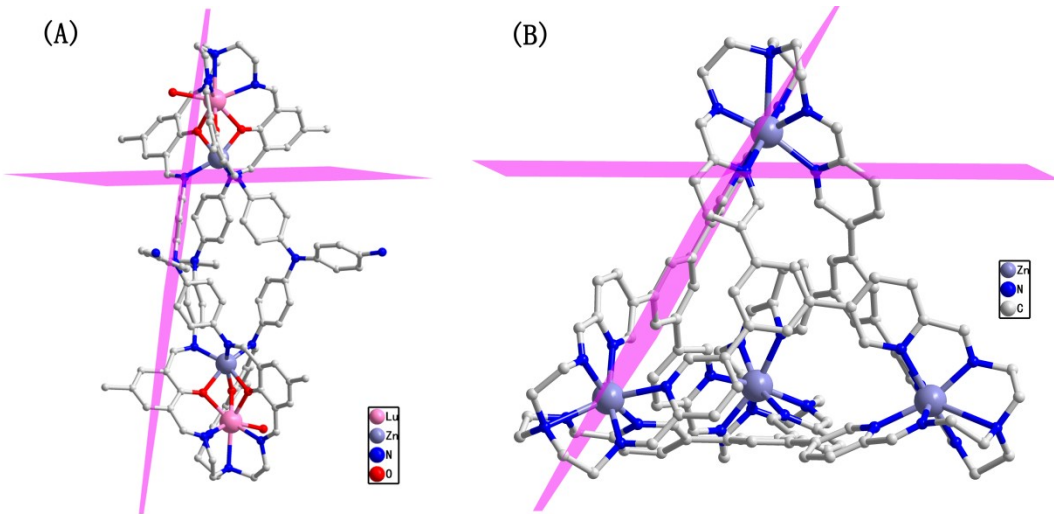


Figure S62. The dihedral angle generated by the plane of three coordinated nitrogen atom closest to panel backbone and one benzene ring plane for **3c-(Lu, Zn)** (A) and reported Zn_4 tetrahedron (B).

Table S1. Crystal data and structure refinement for **3a-(Lu, Zn) and **3b-(Lu, Zn)****

Identification code	3a-(Lu, Zn)	3b-(Lu, Zn)
Empirical formula	C ₇₆ H ₈₆ F ₉ Lu ₂ N ₁₄ O ₁₈ S ₃ Zn ₂	C ₁₁₁ H ₁₀₄ F ₁₂ Lu ₂ N ₁₄ O ₂₀ S ₄ Zn ₂
Formula weight	2231.44	2791.00
Temperature	150(2) K	159.98 K
Wavelength	0.71073 Å	0.71073 Å
Crystal system	Monoclinic	Monoclinic
Space group	C2/c	C2/c
a/Å	36.125(3)	20.602(2)
b/Å	25.6979(18)	26.315(2)
c/Å	26.505(4)	28.155(2)
α/°	90	90
β/°	122.641(2)	93.285(4)
γ/°	90	90
Volume	20719(4) Å ³	15239(2) Å ³
Z	8	4
Density (calculated)	1.431 Mg/m ³	1.217 Mg/m ³
Absorption coefficient	2.485 mm ⁻¹	1.720 mm ⁻¹
F(000)	8920	5608
Crystal size	0.15 x 0.11 x 0.06 mm ³	0.25 x 0.12 x 0.1 mm ³
Theta range for data collection	2.236 to 25.027°.	2.611 to 22.002°.
Index ranges	-42<=h<=42, -30<=k<=30, -29<=l<=31	-20<=h<=21, -27<=k<=27, -29<=l<=29
Reflections collected	144292	47081
Independent reflections	18264 [R(int) = 0.0751]	9273 [R(int) = 0.0866]
Refinement method	Full-matrix least-squares on F ²	Full-matrix least-squares on F ²
Data / restraints / parameters	18264 / 298 / 1180	9273 / 787 / 826
Goodness-of-fit on F ²	1.040	1.022
Final R indices [I>2sigma(I)]	R1 = 0.0473, wR2 = 0.1188	R1 = 0.0815, wR2 = 0.2040
R indices (all data)	R1 = 0.0729, wR2 = 0.1393	R1 = 0.1151, wR2 = 0.2315
Extinction coefficient	n/a	n/a
Largest diff. peak and hole	2.329 and -1.514 e.Å ⁻³	1.426 and -0.966 e.Å ⁻³

Table S2. Crystal data and structure refinement for **3c-(Lu, Zn)** and **3a'-(Dy, Co)**

Identification code	3c-(Lu, Zn)	3a'-(Dy, Co)
Empirical formula	C ₁₂₈ H ₁₂₆ F ₉ Lu ₂ N ₂₀ O ₂₀ S ₃ Zn ₂	C ₇₇ H ₈₃ F ₉ Dy ₂ N ₁₅ O ₁₆ S ₃ Co ₂
Formula weight	3012.34	2184.62
Temperature	170(2) K	150(2) K
Wavelength	0.71073 Å	0.71073 Å
Crystal system	Triclinic	Monoclinic
Space group	P-1	C2/c
a/Å	16.624(3)	35.900(4)
b/Å	21.239(3)	25.827(3)
c/Å	25.607(4)	26.793(5)
α/°	79.242(3)	90
β/°	81.468(4)	123.682(3)
γ/°	70.737(4)	90
Volume	8348(2) Å ³	20671(5) Å ³
Z	2	8
Density (calculated)	1.198 Mg/m ³	1.404 Mg/m ³
Absorption coefficient	1.561 mm ⁻¹	1.882 mm ⁻¹
F(000)	3050	8744
Crystal size	0.03 x 002 x 0.01 mm ³	0.13 x 0.09 x 0.05 mm ³
Theta range for data collection	2.318 to 19.782°.	2.218 to 20.866°.
Index ranges	-15<=h<=15, -20<=k<=20, -24<=l<=24	-35<=h<=35, -25<=k<=25, -26<=l<=26
Reflections collected	54390	99570
Independent reflections	14647 [R(int) = 0.1917]	10829 [R(int) = 0.0531]
Refinement method	Full-matrix least-squares on F ²	Full-matrix least-squares on F ²
Data / restraints / parameters	14647 / 5310 / 1575	10829 / 266 / 1152
Goodness-of-fit on F ²	0.937	1.075
Final R indices [I>2sigma(I)]	R1 = 0.0673, wR2 = 0.1491	R1 = 0.0498, wR2 = 0.1282
R indices (all data)	R1 = 0.1293, wR2 = 0.1778	R1 = 0.0644, wR2 = 0.1443
Extinction coefficient	n/a	n/a
Largest diff. peak and hole	0.786 and -0.994 e.Å ⁻³	2.422 and -1.617 e.Å ⁻³

Table S3. Selected bond distances (\AA) and angles ($^\circ$) for **3a-(Lu, Zn)**

Zn1-O3	2.067(5)	Zn2-O5	2.037(5)
Zn1-N7	2.075(5)	Zn2-N9	2.082(6)
Zn1-N5	2.113(5)	Zn2-N10	2.164(5)
Zn1-O2	2.151(4)	Zn2-O7	2.191(4)
Zn1-O4	2.167(4)	Zn2-N8	2.221(5)
Zn1-N6	2.196(6)	Zn2-O6	2.255(4)
Zn1-Lu1	3.2057(9)	Zn2-Lu2	3.2482(9)
Lu1-O3	2.217(4)	Lu2-O6	2.221(5)
Lu1-O4	2.237(4)	Lu2-O5	2.244(5)
Lu1-O2	2.329(5)	Lu2-O7	2.305(5)
Lu1-O1	2.331(5)	Lu2-O8	2.322(5)
Lu1-N2	2.383(6)	Lu2-N12	2.385(7)
Lu1-N3	2.423(6)	Lu2-N14	2.421(6)
Lu1-N4	2.507(7)	Lu2-N13	2.476(6)
Lu1-N1	2.601(7)	Lu2-N11	2.563(6)
O3-Zn1-O2	73.18(18)	O5-Zn2-O7	73.24(18)
O3-Zn1-O4	78.03(18)	O5-Zn2-O6	75.52(18)
O2-Zn1-O4	73.33(16)	O7-Zn2-O6	71.69(17)
O3-Zn1-N6	81.3(2)	O5-Zn2-N8	82.5(2)
N5-Zn1-O2	86.61(18)	N9-Zn2-O6	81.84(19)
N7-Zn1-O4	84.55(18)	O7-Zn2-N10	84.88(19)
O3-Lu1-O4	73.53(16)	O6-Lu2-O5	72.30(17)
O3-Lu1-O2	67.12(17)	O6-Lu2-O7	70.23(17)
O4-Lu1-O2	68.72(15)	O5-Lu2-O7	67.42(16)
O2-Lu1-N2	70.32(17)	O5-Lu2-N12	74.53(19)
O3-Lu1-N3	73.72(18)	O7-Lu2-N14	70.82(18)
O4-Lu1-N4	74.09(17)	O6-Lu2-N13	74.52(18)
Zn1-O2-Lu1	91.29(17)	Zn2-O5-Lu2	98.6(2)
Zn1-O3-Lu1	96.81(18)	Lu2-O6-Zn2	93.07(18)
Zn1-O4-Lu1	93.41(16)	Zn2-O7-Lu2	92.47(17)
N5-Zn1-O4	159.84(19)	O5-Zn2-N9	157.3(2)
O2-Zn1-N6	154.3(2)	N10-Zn2-O6	156.57(19)
O3-Zn1-N7	162.44(19)	O7-Zn2-N8	155.45(19)

Table S4. Selected bond distances (\AA) and angles ($^\circ$) for **3b-(Lu, Zn)**

Zn1-O2	2.074(8)	Lu1-N4	2.464(12)
Zn1-N7	2.086(11)	Lu1-O2	2.253(8)
Zn1-O1	2.154(7)	Lu1-O1	2.284(8)
Zn1-N5	2.153(9)	Lu1-O4	2.377(9)
Zn1-N6	2.154(9)	Lu1-N1	2.642(12)
Zn1-O3	2.285(8)	Lu1-N2	2.412(10)
Zn1-Lu1	3.2408(13)	Lu1-N3	2.400(15)

Lu1-O3	2.239(8)	Lu1-O3-Zn1	91.5(3)
O3-Lu1-O2	73.4(3)	O2-Zn1-O1	72.7(3)
O3-Lu1-O1	71.6(3)	O2-Zn1-O3	75.9(3)
O2-Lu1-O1	67.1(3)	O1-Zn1-O3	73.1(3)
O2-Lu1-N3	72.9(4)	O1-Zn1-N5	85.3(3)
O1-Lu1-N2	71.1(3)	O2-Zn1-N6	83.1(3)
O3-Lu1-N4	74.7(3)	N7-Zn1-O3	83.6(4)
N5-Zn1-O3	158.3(3)	Zn1-O1-Lu1	93.8(3)
O2-Zn1-N7	159.5(4)	Zn1-O2-Lu1	96.9(4)
N6-Zn1-O1	155.8(3)		

Table S5. Selected bond distances for **3c-(Lu, Zn)**

Lu1-O3	2.225(8)	Lu2-O6	2.210(10)
Lu1-O2	2.224(10)	Lu2-O5	2.242(10)
Lu1-O1	2.309(10)	Lu2-O7	2.342(12)
Lu1-O4	2.319(9)	Lu2-N17	2.402(15)
Lu1-N3	2.386(13)	Lu2-N18	2.416(17)
Lu1-N2	2.402(12)	Lu2-O8	2.380(13)
Lu1-N4	2.410(11)	Lu2-N19	2.471(13)
Lu1-N1	2.595(12)	Lu2-N20	2.581(14)
Lu1-Zn1	3.2572(18)	Lu2-Zn2	3.248(2)
Zn1-O2	2.055(9)	Zn2-O5	2.061(11)
Zn1-N5	2.100(11)	Zn2-N16	2.084(13)
Zn1-N6	2.141(14)	Zn2-O7	2.120(11)
Zn1-N7	2.156(11)	Zn2-N15	2.147(13)
Zn1-O1	2.155(10)	Zn2-N14	2.158(14)
Zn1-O3	2.286(10)	Zn2-O6	2.281(9)
O3-Lu1-O2	72.8(3)	O6-Lu2-O5	73.3(4)
O3-Lu1-O1	70.6(3)	O6-Lu2-O7	70.8(4)
O2-Lu1-O1	66.4(3)	O5-Lu2-O7	65.4(4)
O3-Lu1-N2	76.0(4)	O5-Lu2-N27	73.9(4)
O1-Lu1-N3	70.9(4)	O7-Lu2-N18	71.0(4)
O2-Lu1-O4	74.5(4)	O6-Lu2-N19	76.0(4)
O2-Zn1-O3	74.7(4)	O5-Zn2-O6	75.3(4)
O2-Zn1-O1	71.9(4)	O7-Zn2-O6	73.6(4)
O1-Zn1-O3	72.6(4)	O5-Zn2-O7	72.7(5)
N6-Zn1-O1	84.4(4)	O5-Zn2-N14	82.1(5)
N5-Zn1-O3	83.8(4)	N16-Zn2-O6	83.0(4)
O2-Zn1-N7	84.3(4)	O7-Zn2-N15	85.5(5)
Zn1-O1-Lu1	93.7(4)	Zn2-O5-Lu2	97.9(5)
Zn1-O2-Lu1	99.1(4)	Lu2-O6-Zn2	92.6(4)
Lu1-O3-Zn1	92.4(3)	Zn2-O7-Lu2	93.3(5)

Table S6. Selected bond distances for **3a'**-(Dy, Co)

Co1-O3	2.131(7)	Co2-O5	2.116(6)
Co1-O2	2.189(6)	Co2-O6	2.268(6)
Co1-N7	2.195(7)	Co2-O7	2.220(6)
Co1-O4	2.207(5)	Co2-N8	2.321(7)
Co1-N5	2.210(7)	Co2-N9	2.188(8)
Co1-N6	2.293(7)	Co2-N10	2.247(7)
Co1-Dy1	3.2365(15)	Co2-Dy2	3.2727(15)
Dy1-O3	2.263(6)	Dy2-O5	2.277(6)
Dy1-O4	2.292(6)	Dy2-O6	2.286(7)
Dy1-O2	2.374(6)	Dy2-O7	2.345(6)
Dy1-O1	2.417(7)	Dy2-O8	2.384(6)
Dy1-N2	2.428(8)	Dy2-N11	2.598(8)
Dy1-N3	2.470(7)	Dy2-N12	2.432(8)
Dy1-N4	2.507(7)	Dy2-N13	2.509(7)
Dy1-N1	2.601(7)	Dy2-N14	2.449(8)
O3-Co1-O2	73.4(2)	O5-Co2-O6	77.2(2)
O3-Co1-O4	79.7(2)	O5-Co2-O7	73.9(2)
O2-Co1-O4	74.9(2)	O7-Co2-O6	73.3(2)
O2-Co1-N5	83.5(2)	O5-Co2-N8	79.7(3)
O3-Co1-N6	78.0(3)	N9-Co2-O6	79.9(2)
N7-Co1-O4	82.1(2)	O7-Co2-N10	82.2(2)
O3-Dy1-O2	75.3(2)	O5-Dy2-O6	73.7(2)
O3-Dy1-O4	67.6(2)	O5-Dy2-O7	68.7(2)
O4-Dy1-O2	69.9(2)	O6-Dy2-O7	70.7(2)
O2-Dy1-N2	70.1(2)	O5-Dy2-N12	73.7(2)
O3-Dy1-N3	74.0(2)	O7-Dy2-N14	70.7(2)
O4-Dy1-N4	73.0(2)	O6-Dy2-N13	73.5(2)
Co1-O2-Dy1	90.3(2)	Co2-O5-Dy2	96.2(2)
Co1-O3-Dy1	94.8(2)	Co2-O6-Dy2	91.9(2)
Co1-O4-Dy1	92.0(2)	Co2-O7-Dy2	91.6(2)

7. Continuous shape measurements analysis

A continuous shape measures (CShMs) analysis of Lu and Zn coordination polyhedra present in the asymmetric unit of **3a-3c-(Lu, Zn)** and Dy and Co coordination polyhedra present in the asymmetric unit of **3a'-(Dy, Co)** has been performed with the SHAPE 2.1 software considering an eight-coordination or six-coordination⁵ (Table S7 and Table S8).

Table S7. Coordination geometries of Ln^{III} evaluated by SHAPE 2.1 considering an eight-coordination.

Abbreviation	Symmetry	Ideal geometry
OP-8	D_{8h}	Octagon
HPY-8	C_{7v}	Heptagonal pyramid
HBPY-8	D_{6h}	Hexagonal bipyramid
CU-8	O_h	Cube
SAPR-8	D_{4d}	Square antiprism
TDD-8	D_{2d}	Triangular dodecahedron
JGBF-8	D_{2d}	Johnson gyrobifastigium J26
JETBPY-8	D_{3h}	Johnson elongated triangular bipyramid J14
JBTPR-8	C_{2v}	Biaugmented trigonal prism J50
BTPR-8	C_{2v}	Biaugmented trigonal prism
JSD-8	D_{2d}	Snub disphenoid
TT-8	T_d	Triakis tetrahedron
ETBPY-8	D_{3h}	Elongated trigonal bipyramid

Table S8. Coordination geometries of Zn^{II} or Co^{II} evaluated by SHAPE 2.1 considering a six-coordination.

Abbreviation	Symmetry	Ideal geometry
HP-6	D_{6h}	Hexagon
PPY-6	C_{5v}	Pentagonal pyramid
OC-6	O_h	Octahedron
TPR-6	D_{3h}	Trigonal prism
JPPY-6	C_{5v}	Johnson pentagonal pyramid J2

Table S9. Coordination geometries of Ln^{III} outputted by SHAPE 2.1 software.

Ln Center	OP-8	HPY-8	HBPY-8	CU-8	SAPR-8	TDD-8	JGBF-8	JETBPY-8	JBTPR-8	BTPR-8	JSD-8	TT-8	ETBPY-8
3a-(Lu, Zn)													
Lu1	32.499	21.433	14.751	13.409	4.349	1.990	9.836	26.432	3.328	2.502	3.541	14.037	21.218
Lu2	31.872	21.088	15.188	13.223	3.664	1.870	10.370	26.243	3.347	2.563	3.374	13.853	21.026
3b-(Lu, Zn)													
Lu1	32.432	21.722	14.435	13.711	4.048	1.930	9.595	26.277	3.370	2.749	3.402	14.313	21.517
3c-(Lu, Zn)													
Lu1	31.557	21.658	14.918	13.297	3.633	1.650	10.216	26.460	3.304	2.654	3.218	14.006	21.818
Lu2	32.158	21.613	14.757	13.600	3.950	1.857	9.873	26.144	3.387	2.582	3.293	14.263	21.055
3a'-(Dy, Co)													
Dy1	32.862	21.356	14.511	13.577	4.239	1.971	9.678	26.476	3.478	2.574	3.617	14.235	21.369
Dy2	31.720	20.768	15.019	13.109	3.482	1.936	10.375	25.815	3.546	2.755	3.579	13.761	20.539

Table S10. Coordination geometries of Zn^{II} or Co^{II} outputted by SHAPE 2.1 software.

Metal	HP-6	PPY-6	OC-6	TPR-6	JPPY-6
3a-(Lu, Zn)					
Zn1	33.142	24.196	2.263	10.984	28.438
Zn2	33.717	24.575	2.595	11.152	28.210
3b-(Lu, Zn)					
Zn1	33.409	24.265	2.474	9.994	27.804
3c-(Lu, Zn)					
Zn1	33.146	23.537	2.934	8.972	26.872
Zn2	32.963	23.168	3.042	8.718	26.586
3a'-(Dy, Co)					
Co1	33.750	22.687	3.199	9.468	26.480
Co2	34.216	23.334	3.127	10.391	27.577

7. Reference

1. Z. Asadi, M. Golchin, V. Eigner, M. Dusek and Z. Amirghofran, *Inorg. Chim. Acta*, 2017, **465**, 50.
2. C. D. Buch, S. H. Hansen, C. M. Tram, D. Mitcov and S. Piligkos, *Inorg. Chem.*, 2020, **59**, 16328.
3. G. M. Sheldrick, *Acta Crystallogr C Struct Chem*, 2015, **71**, 3.
4. A. L. Spek, *Appl. Crystallogr.*, 2003, **36**, 7.
5. D. Casanova, M. Llunell, P. Alemany and S. Alvarez, *Chem. Eur. J.*, 2005, **11**, 1479.